# Availability, Feasibility, and Reliability of Available Nondestructive Evaluation (NDE) Technologies for Detecting and Locating Buried Utilities: Final Report

PUBLICATION NO. FHWA-HRT-23-037

JULY 2023


U.S. Department of Transportation
**Federal Highway Administration**

Research, Development, and Technology
Turner-Fairbank Highway Research Center
6300 Georgetown Pike
McLean, VA 22101-2296

Long-Term
Bridge Performance
Program

## FOREWORD

This final report presents the use of promising nondestructive evaluation (NDE) and geophysical techniques for the detection of buried underground utilities. The project was conducted in stages, including a literature review, controlled laboratory testing, and field experiments to assess performance under real-world conditions. As a result of this research, a new module will be added to Federal Highway Administration (FHWA) InfoTechnology web portal.

Bridge and pavement owners, consultants, contractors, and technical experts interested in underground utilities are expected to benefit from the information contained herein.

Jean A. Nehme, Ph.D., P.E.
Director, Office of Infrastructure
Research and Development

# TECHNICAL REPORT DOCUMENTATION PAGE

| 1. Report No.<br>FHWA-HRT-23-037 | 2. Government Accession No. | 3. Recipient's Catalog No. |
|---|---|---|
| 4. Title and Subtitle<br>Availability, Feasibility, and Reliability of Available Nondestructive Evaluation (NDE) Technologies for Detecting and Locating Buried Utilities: Final Report | | 5. Report Date<br>July 2023 |
| | | 6. Performing Organization Code: |
| 7. Author(s)<br>Delaine Reiter, Vanessa Napoli, Jeff Cohen, Shane Boone, Patrick Moseley, Ahmad Alhasan, Jeremy Salerno | | 8. Performing Organization Report No. |
| 9. Performing Organization Name and Address<br>Applied Research Associates<br>4300 San Mateo Blvd, NE, Ste. 200<br>Albuquerque, NM 87110 | | 10. Work Unit No. |
| | | 11. Contract or Grant No.<br>693JJ320C000005 |
| 12. Sponsoring Agency Name and Address<br>Office of Infrastructure Research and Development<br>Federal Highway Administration<br>6300 Georgetown Pike<br>McLean, VA 22101-2296 | | 13. Type of Report and Period Covered<br>Final Report: April 2020–August 2022 |
| | | 14. Sponsoring Agency Code<br>HRDI-30 |
| 15. Supplementary Notes<br>The Contracting Officer's Representative was Frank Jalinoos (HRDI-30), ORCID: 0000-0001-8330-7603 | | |
| 16. Abstract<br>Modern nondestructive evaluation (NDE) technologies offer an expanding suite of geophysical techniques to detect and locate buried utilities. This project focused on identifying promising technologies that merit expanded application and mainstream deployment by State transportation departments. The project team applied a staged approach to the effort, which included a thorough review of the open scientific literature, controlled testing of candidate NDE technologies, and field experiments to assess performance under real-world conditions. | | |
| 17. Key Words<br>Nondestructive evaluation, buried utility detection and location | | 18. Distribution Statement<br>No restrictions. This document is available to the public through the National Technical Information Service, Springfield, VA 22161.<br>http://www.ntis.gov |

| 19. Security Classif. (of this report)<br>Unclassified | 20. Security Classif. (of this page)<br>Unclassified | 21. No. of Pages<br>70 | 22. Price<br>N/A |
|---|---|---|---|

**Form DOT F 1700.7 (8-72)** Reproduction of completed page authorized.

## SI* (MODERN METRIC) CONVERSION FACTORS

### APPROXIMATE CONVERSIONS TO SI UNITS

| Symbol | When You Know | Multiply By | To Find | Symbol |
|---|---|---|---|---|
| | | **LENGTH** | | |
| in | inches | 25.4 | millimeters | mm |
| ft | feet | 0.305 | meters | m |
| yd | yards | 0.914 | meters | m |
| mi | miles | 1.61 | kilometers | km |
| | | **AREA** | | |
| $in^2$ | square inches | 645.2 | square millimeters | $mm^2$ |
| $ft^2$ | square feet | 0.093 | square meters | $m^2$ |
| $yd^2$ | square yard | 0.836 | square meters | $m^2$ |
| ac | acres | 0.405 | hectares | ha |
| $mi^2$ | square miles | 2.59 | square kilometers | $km^2$ |
| | | **VOLUME** | | |
| fl oz | fluid ounces | 29.57 | milliliters | mL |
| gal | gallons | 3.785 | liters | L |
| $ft^3$ | cubic feet | 0.028 | cubic meters | $m^3$ |
| $yd^3$ | cubic yards | 0.765 | cubic meters | $m^3$ |
| | | **NOTE**: volumes greater than 1,000 L shall be shown in $m^3$ | | |
| | | **MASS** | | |
| oz | ounces | 28.35 | grams | g |
| lb | pounds | 0.454 | kilograms | kg |
| T | short tons (2,000 lb) | 0.907 | megagrams (or "metric ton") | Mg (or "t") |
| | | **TEMPERATURE (exact degrees)** | | |
| °F | Fahrenheit | 5 (F-32)/9<br>or (F-32)/1.8 | Celsius | °C |
| | | **ILLUMINATION** | | |
| fc | foot-candles | 10.76 | lux | lx |
| fl | foot-Lamberts | 3.426 | $candela/m^2$ | $cd/m^2$ |
| | | **FORCE and PRESSURE or STRESS** | | |
| lbf | poundforce | 4.45 | newtons | N |
| $lbf/in^2$ | poundforce per square inch | 6.89 | kilopascals | kPa |

### APPROXIMATE CONVERSIONS FROM SI UNITS

| Symbol | When You Know | Multiply By | To Find | Symbol |
|---|---|---|---|---|
| | | **LENGTH** | | |
| mm | millimeters | 0.039 | inches | in |
| m | meters | 3.28 | feet | ft |
| m | meters | 1.09 | yards | yd |
| km | kilometers | 0.621 | miles | mi |
| | | **AREA** | | |
| $mm^2$ | square millimeters | 0.0016 | square inches | $in^2$ |
| $m^2$ | square meters | 10.764 | square feet | $ft^2$ |
| $m^2$ | square meters | 1.195 | square yards | $yd^2$ |
| ha | hectares | 2.47 | acres | ac |
| $km^2$ | square kilometers | 0.386 | square miles | $mi^2$ |
| | | **VOLUME** | | |
| mL | milliliters | 0.034 | fluid ounces | fl oz |
| L | liters | 0.264 | gallons | gal |
| $m^3$ | cubic meters | 35.314 | cubic feet | $ft^3$ |
| $m^3$ | cubic meters | 1.307 | cubic yards | $yd^3$ |
| | | **MASS** | | |
| g | grams | 0.035 | ounces | oz |
| kg | kilograms | 2.202 | pounds | lb |
| Mg (or "t") | megagrams (or "metric ton") | 1.103 | short tons (2,000 lb) | T |
| | | **TEMPERATURE (exact degrees)** | | |
| °C | Celsius | 1.8C+32 | Fahrenheit | °F |
| | | **ILLUMINATION** | | |
| lx | lux | 0.0929 | foot-candles | fc |
| $cd/m^2$ | candela/m2 | 0.2919 | foot-Lamberts | fl |
| | | **FORCE and PRESSURE or STRESS** | | |
| N | newtons | 2.225 | poundforce | lbf |
| kPa | kilopascals | 0.145 | poundforce per square inch | $lbf/in^2$ |

*SI is the symbol for International System of Units. Appropriate rounding should be made to comply with Section 4 of ASTM E380. (Revised March 2003)

## TABLE OF CONTENTS

## LIST OF FIGURES

## LIST OF TABLES

## LIST OF ABBREVIATIONS

| | |
|---|---|
| 1D | one-dimensional |
| 2D | two-dimensional |
| 3D | three-dimensional |
| AC | alternating current |
| APL | acoustic pipe locator |
| DF | dual frequency |
| DOT | department of transportation |
| EM | electromagnetic |
| FDEM | frequency-domain electromagnetic |
| FHWA | Federal Highway Administration |
| GPR | ground-penetrating radar |
| GPS | Global Positioning System |
| HVSR | horizontal-to-vertical spectral ratio |
| MASW | multichannel analysis of surface waves |
| NDE | nondestructive evaluation |
| PVC | polyvinyl chloride |
| SASW | spectral analysis of surface waves |
| SHRP 2 | Second Strategic Highway Research Program |
| TDEM | time-domain electromagnetic |
| VDOT | Virginia Department of Transportation |
| $V_s$ | shear velocity |

## EXECUTIVE SUMMARY

Modern nondestructive evaluation (NDE) technologies offer an expanding suite of geophysical techniques to detect and locate buried utilities. This project focused on identifying promising technologies that merit expanded application and mainstream deployment by State transportation departments. The project team applied a staged approach to the effort, which included a thorough review of the open scientific literature, controlled testing of candidate NDE technologies, and field experiments to assess performance under real-world conditions.

The literature review identified several current and emerging NDE technologies that could improve the detection and location of underground utilities across four geophysical domains: magnetic technologies, electromagnetic (EM) technologies, acoustic technologies, and seismic technologies. The project team gathered capability information for NDE mapping techniques across a diverse array of conditions and applications. Some of the identified NDE technologies, such as traditional ground-penetrating radar (GPR) methods and pile-and-cable locators, have already been broadly deployed in subsurface utilities location projects. Other technologies, such as stepped-frequency GPR and multichannel analysis of surface waves (MASW), show increasing promise in field tests and continue to undergo improvements in data acquisition and high-resolution mapping.

In the second phase of the project, the team assessed the capabilities of NDE technologies under controlled laboratory conditions to establish performance baselines and compare the strengths and weaknesses of each technique. To accomplish this, the project team built a set of soil-filled enclosures and emplaced utility pipes of varied types, depths, and diameters in different soil conditions and burial configurations. NDE technologies from the four geophysical domains were tested to determine their baseline characteristics in the soil enclosures. GPR was found to be the most effective of all the methods tested in this (test bed) environment because it was successfully able to locate both polyvinyl chloride (PVC) and metallic pipes down to a 6-ft depth.

The last phase of the project included real-world field tests of five NDE technologies at sites having well-documented locations of buried utilities with different material types and emplacement conditions. The results showed GPR remains the most reliable and consistent NDE method available for the buried utility application. MASW proved to be an emerging NDE technology that successfully located buried utilities at one of the field sites. Frequency-domain EM sensors, passive pipe locators, and the acoustic pipe locator failed to identify such targets reliably.

In summary, this comprehensive survey of existing and emerging NDE technologies identified stepped-frequency GPR and MASW as versatile and promising NDE technologies for detecting and locating buried utilities.

# CHAPTER 1. INTRODUCTION

Underground utilities represent fundamental assets in the infrastructure network of each city and State, providing essential services, such as water, gas, sewage, telecommunications, and power, to their populations. The loss of such services due to outages can have significant and even fatal consequences. Outages can occur due to integrity loss in the utility lines themselves or through unintended damage and disruption caused by construction activities. Infrastructure construction and renovation activities also necessitate the identification, characterization, and relocation of subsurface utility lines. Minimizing outages and service disruptions is a difficult task, especially for highway agencies that may not have regular lines of communication established with local utility providers.

Furthermore, managing complex arrays of utility networks is challenging because underground utilities are often buried in public urban areas (roads, streets, etc.) without accurate metadata on the location, orientation, and types of underground utility lines present. In the absence of comprehensive utility location maps, traditional utility location methods rely on physical verification through time-consuming open-cuts practices (excavations, trenches, etc.) that interfere with tightly scheduled project activities and can damage the underground utilities and surrounding areas. As a result, the Federal Highway Administration (FHWA) has identified a critical need to investigate the availability, feasibility, and reliability of existing nondestructive evaluation (NDE) technologies to locate buried utilities and develop a comprehensive procedure for deploying appropriate NDE systems for use in a variety of settings and configurations.

FHWA has already engaged in multiple projects to address this need within the industry, assessing the effectiveness of certain NDE technologies and collecting significant feedback from State departments of transportation (DOTs) on their utility location challenges and current solutions. The Second Strategic Highway Research Program (SHRP 2) produced several reports that explored electromagnetic (EM), infrared, elastic, and other geophysical technologies for their use in detecting, locating, and characterizing subsurface utilities (Sterling et al. 2009; Young and Kennedy 2015). This work provided a foundation on which to incorporate the current and emerging technologies the NDE industry has to offer for utility location.

The current project focused on existing technologies that have benefited from significant technological improvements since SHRP 2, such as the following:

- Stepped-frequency ground-penetrating radar (GPR)—GPR is a geophysical NDE technique that uses EM signals to detect and identify subsurface anomalies based on changes in electrical conductivity and relative dielectric properties of the subsurface layers. Stepped-frequency GPR has been developed in recent years to address these challenges. Rather than relying on a single-frequency antenna, stepped-frequency GPR systems combine an array of multiple smaller antennas that sweep through a wide frequency range to provide an effective balance of depth and precision in measurement of subsurface features (Metje et al. 2007). While stepped-frequency GPR has been improved significantly and developed into a commercial product during the last two decades, availability and affordability of vehicle-mounted units have presented major roadblocks to adopting this technology. However, additional product suppliers have recently entered

the market with competitively priced cart-based systems. Furthermore, recently developed software enhancements supporting this technology now provide automated analysis tools that require less extensive operator training to deploy stepped-frequency GPR systems successfully.

- Acoustic/elastic-wave techniques—A variety of seismic and acoustic methods exist to detect and locate shallow subsurface features. Older techniques (active, passive, and resonant sonics; seismic refraction/reflection) cannot provide the high subsurface resolution of GPR, but newer methods hold some promise for improved outcomes, especially when combined with GPR surveys. For example, the multichannel analysis of surface waves (MASW) method generates cross-sectional, inverted shear images of the ground from surface waves propagated between an active seismic source and geophone receivers at predetermined offsets (Datta and Sarkar 2016; Hawari et al. 2017). Brand new techniques, such as distributed acoustic sensing using fiber optic cables, may eventually have a strong impact on the detection, location, and real-time monitoring of buried utilities (Hutchinson and Beird 2016; Khalil, Anukwu, and Nordin 2020).

- Magnetic detection—This technique measures the anomalies in the Earth's magnetic field caused by buried metallic power cables as a means to locate them. It can be challenging to locate individual cables in the presence of superimposed magnetic fields or interferences from different cables buried in the same area. Conventional cable avoidance tool devices have been used successfully to locate buried power cables as long as there is minimal interference from nearby cables and metallic utilities (Metje et al. 2007).

- Frequency-domain electromagnetic (FDEM) method and time-domain electromagnetic (TDEM) method—FDEM and TDEM represent two different technical approaches for completing terrain conductivity surveys by using EM wavefields to detect differences in average conductivity between utilities and surrounding soils to locate underground facilities. FDEM sweeps through a spectrum of frequencies to measure conductivity at a range of depths. TDEM uses a specialized periodic current to send out a single impulse that allows for deeper scans of the terrain to be performed. TDEM tends to be robust in the face of minor soil variations, while FDEM tends to be more sensitive with the capability to measure a feature depth based on the frequency sweep (Wightman et al. 2003). Terrain conductivity surveying is useful for utility detection in areas of high ambient conductivity (Anspach 1995). It can detect a wide range of metallic utilities, such as underground storage tanks, vault covers, wells, and other isolated metallic utilities buried up to 16.4 ft deep (ASCE 2002). The performance of terrain conductivity imaging can be affected considerably by interfering magnetic fields produced along overhead power lines and by above-ground metal objects, such as vehicles, fences, or buildings (Jeong and Abraham 2004), and the physical and chemical properties of the surrounding soils. TDEM was also used as part of a vehicle-mounted system in the 2009 SHRP 2 study.

The project team evaluated several of these NDE technologies for their technical capabilities and feasibility in addressing the buried utility location problem.

# CHAPTER 2. CANDIDATE NDE TECHNOLOGIES TO DETECT AND LOCATE BURIED UTILITIES

The following section summarizes a comprehensive literature review of promising NDE technologies for buried utility detection and location. NDE technologies that rely on EM wavefields to probe the subsurface, such as GPR and TDEM/FDEM, continue to be the most widely used for the buried utility application. Each technology exhibits both strengths and limitations in survey cost and time that depend on the setting and other factors. In contrast, seismic and acoustic technologies are not widely used for NDE utility detection. However, the open scientific literature indicates that seismic and acoustic methods can be combined successfully with GPR and EM methods to reduce location uncertainty. Furthermore, seismic and acoustic technologies are particularly useful when GPR and EM surveys fail due to soil saturation, conductivity issues, physical surface obstructions, or pipe material. Table 1 summarizes the reviewed NDE technologies, including their advantages, automation potential, and related issues and limitations.

## EM METHODS

### GPR

GPR is a geophysical method developed for high-resolution investigations of Earth's shallow subsurface and other structural systems. GPR operates by transmitting short pulses of EM energy into a material using an antenna attached to a scanning system. The pulses reflect off dielectric discontinuities in the material and are recorded by a receiving antenna. Reflection arrival times and amplitudes relate directly to the location and nature of the dielectric discontinuities (e.g., air-to-asphalt or asphalt-to-concrete, reinforcing steel, and underground utility). An oscilloscope displays the reflected energy captured by the GPR antenna as a series of pulses known as the "radar signal." Each radar signal records the properties and thicknesses of the layers within the subsurface beneath the transmitting antenna. By combining multiple sampled signals from a moving survey into a single image, features within a structure can be identified.

Since the 1970s, applications of GPR have expanded to several areas, including the following:

- Environmental and agricultural monitoring (Hubbard et al. 2005).
- Sedimentary study (Neal 2004).
- Forensic investigation (Hammon III, McMechan, and Zeng 2000).
- Glacier monitoring (Hamran et al. 1997; Plewes and Hubbard 2001; Moorman and Michel 2000; Hamran and Langley 2004).
- Landmine detection (Daniels 2004; Langman and Inggs 1998; Scheers, Piette, and Vander Vorst 1998).
- Archaeological investigations (Sciotti et al. 2003).
- Civil engineering (Grandjean, Gourry, and Bitri 2000; Xiaojian, Haizhong, and Huiliang 1997). Lai, Dérobert, and Annan (2018) provide an extensive review of GPR studies to document underground utilities.

Figure 1 presents a vehicle-mounted GPR scan from this research study in which a buried object (utility pipe) was found. The utility pipe is indicated by the white-black-white patterned hyperbola. GPR can be used for utility service location by identifying these EM boundaries between the soil and other media, such as gas or water pipes, cables, and different soils or voids. The strength and polarity of a GPR echo depend on several factors, including the absorption of the signal as it propagates to the target and back to the radar; the size, shape, and composition of the target; and the strength of the discontinuity at the reflecting boundary (Dolphin 1997).

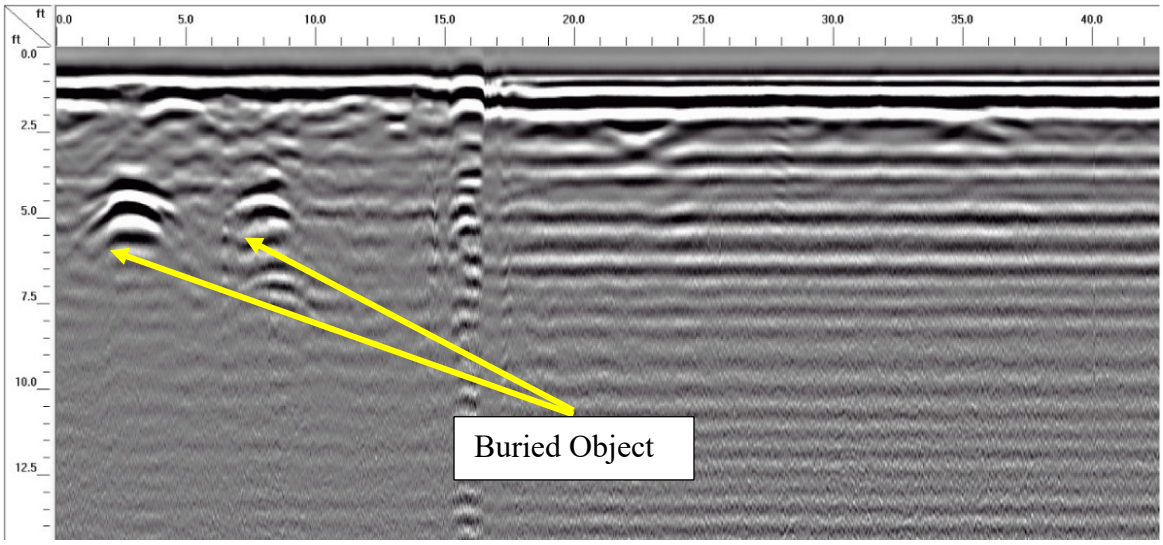


Source: FHWA.

**Figure 1. Image. Single GPR scan compiled by a survey vehicle identifying buried objects, which are indicated by the arrows pointed at the hyperbola.**

### *Single-Frequency Impulse GPR*

Most GPR surveys use the single-frequency impulse GPR system described earlier in this section. Pulsed GPR techniques were developed starting in the 1930s to probe through ice, fresh water, salt deposits, desert sand, and rock formations. Impulse GPR systems have matured since the mid-1970s (Daniels 2004), and they are still of interest to many researchers due to their numerous advantages. Figure 2 presents a theoretical depiction of a traditional single-frequency impulse GPR antenna in operation on a concrete slab with two layers of steel reinforcement, where the resulting scan image is presented with the diagram. The scan image presents the typical hyperbola feature that correlates with pipe-like elements like rebar or utility pipes, where the presence of the top layer partially obscures the bottom layer. Although the impulse GPR is the most used system today, its noisy and inefficient receiver limits overall performance. Several advances have improved impulse GPR performance, including multiantenna (Yarovoy et al. 2003; Manacorda et al. 2004), ultra-short-pulse generator (Park et al. 2003; Park et al. 2004), and multiwaveform designs (Yarovoy et al. 2003; Park et al. 2003). These conventional GPR systems have been used worldwide for underground utility location problems (Jeng and Chen 2012; Metwaly 2015; Jaw and Hashim 2013).

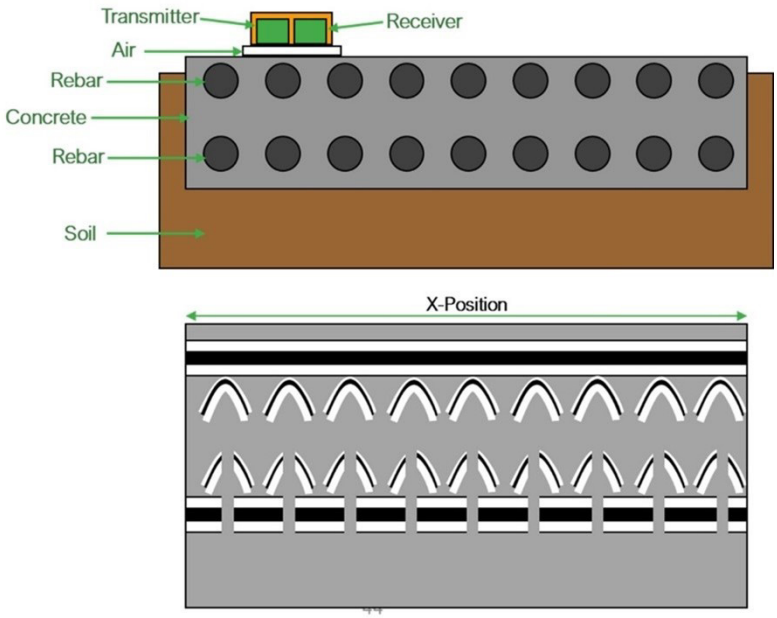


Source: FHWA.

**Figure 2. Illustration. Plan view synthetic data presentation of GPR antenna traveling over concrete with steel reinforcement with B-scan GPR data presented in reference to the scan location.**

### *Stepped-Frequency GPR Systems*

Traditional single-frequency impulse GPR is limited in terms of widespread application and adoption, primarily due to the tradeoff between high measurement precision and useful penetration depth (Kavi 2018). In recent years, stepped-frequency GPR systems have been developed to address these challenges. Rather than relying on a single-frequency antenna, stepped-frequency systems use an array of multiple, smaller antennas used in various combinations to sweep through an entire range of frequencies to get an effective balance of depth and precision in measurement of subsurface features (Metje et al. 2007). Typical stepped-frequency antennas produce a series of impulse bursts across multiple frequencies (typically 100 MHz–3.0 GHz) in a swept sine output fashion. The receiver measures the phase and amplitude from each frequency transmitted to generate a time domain profile that can then be transferred to the frequency domain to generate a plot identifying amplitude reflections from multiple depth layers. Additionally, because these antennas are operated in unison across multiple frequency bands, multiple antennas are typically mounted simultaneously to collect data across more than one single line scan, as performed with a single-frequency impulse GPR. This technique allows for these antennas to be vehicle mounted and collect an entire lane's worth of data in a single pass. Additionally, the antennas can be either air or ground coupled (figure 3).

While stepped-frequency GPR systems have advanced considerably and been developed into a commercial product during the last two decades, system availability and affordability have presented major historical roadblocks to adopting them as a viable NDE technology because the market lacked vendors selling the systems, and their price has not justified their use over traditional systems. However, more vendors have come to market with competitively priced

systems that make stepped-frequency GPR much more logistically and fiscally viable for organizations that have historically been unable to justify the expense. The software supporting this technology also provides additional tools for automated analysis, which means operators may not require extensive training for successful deployment of the system.

Source: FHWA.

**Figure 3. Photo. Air-coupled, step-frequency GPR mounted on a vehicle for underground utility location under roadway.**

### *Multichannel GPR Systems*

Multichannel GPR systems use synchronized, single-channel, bi-static GPR antennas in various array layouts. Similar to multiantenna, stepped-frequency GPR systems, these arrays generally are intended to be used for large-scale, mostly vehicle-mounted, data collection, but some can be uniquely customized to accommodate various project specifications. Multichannel GPR systems have been used for two decades, but early systems did not deliver quality results due to the lack of synchronization of the individual antenna responses. In the last 10 years, this asynchronous response has mostly been solved by technological advancements, and there is now a wider acceptance of multichannel GPR systems in various industries. Deploying a multichannel GPR system can be very effective in finding unknown utilities because it can reduce the survey time significantly and provides high-density data capture with greater resolution. A case study conducted by the New York State DOT on the applications of GPR for highway pavements showed the ability of multichannel GPR technology to detect and map buried utilities, indicating the utility depths, orientations, and proximities to other surrounding infrastructure (Grivas 2006).

## Low-Frequency EM Instruments: Pipe and Cable Locators

Finding a buried utility line is very similar in concept to radio detection: the utility line behaves like a radio station that transmits a signal, and an underground utility locator is used to pick up this signal. This concept was first proposed, studied, and demonstrated by Gerhard Fisher owing

to his work on aircraft radio detection (Chemekoff and Toussaint 1994). With the technological advancement made in this field, a wide variety of underground utility locators now exist, among which are pipe and cable locators. This family of standard EM instruments is used to detect magnetic fields around buried pipes and cables made of conductive materials. A pipe and cable locator can be designed to work either in passive or active modes. In passive mode, the locator listens to the background noise from the utility, and in active mode, the locator listens to a signal introduced into the utility using a transmitter. The transmission involves using coils that create and release EM currents that propagate in the ground and generate magnetic fields around conductive materials.

The magnetic fields induced can be sensed by an EM receiver located on the surface of the ground. For better active detection performance, it is recommended that the transmitter be in the same orientation of the utility. This positioning can be achieved by trial and error. Once the magnetic fields are received, the signals recorded are processed, analyzed, and interpreted to produce and visualize the results indicating the horizontal location of the subsurface utility. The signal produced by the transmitter can be sent through the utility by either conductive means through a direct connection, such as alligator clips, or by inductive means, where the signal is introduced directly onto the metallic utility line using an induction clamp that is secured or clamped around the utility line but does not connect metal to metal as the conductive alligator clip does. The inductive method is great when the utility is not accessible, but the direct (conductive) method is far more reliable because it is less prone to signal distortion and interference from neighboring utilities.

With ideal soil conditions, the effective locating depth of the direct method is about 9.8 ft, but this depth reduces considerably in dry sand and alkaline and high iron-content soils (Jeong and Abraham 2004). The method works well with aluminum, steel pipes, copper, and other metallic utilities that are buried with tracing materials above the utility itself but does not work on nonconductive utilities, such as those made of cast iron. This obstacle can, however, be easily overcome in many cases. For example, in the case a nonconductive pipe is accessible, an insulated trace wire connected to the transmitter can be fished through the pipe. The receiver is then waved close to where the pipe is buried to mark its horizontal location.

Pipe and cable locating instruments use a small yet crucial range of the EM spectrum, with frequencies ranging from about 50 KHz to 480 KHz (ASCE 2002). The instruments can either be single-frequency devices or multifrequency devices, where both have advantages and limitations.

**FDEM Method: Terrain Conductivity Method**

Terrain conductivity surveying is an EM technique that uses the differences in average conductivity between utilities and surrounding soils to locate underground facilities. The technique is based on the principles of eddy currents. A transmitter coil connected to an alternating current (AC) source emits a primary magnetic field that produces induced secondary currents known as eddy currents into the earth directly below the coil. The induced currents flow to the surface with slightly different properties when they encounter a buried object with conductivity different from the surrounding soil. A receiver at the ground uses the differences between the emitted and induced currents to detect underground utilities. For instance, a buried

metallic object has a lower conductivity than the soil surrounding it. Therefore, the induced currents have a different value than the currents emitted.

Terrain conductivity surveying is useful for utility detection in areas of high ambient conductivity (Anspach 1995). It can detect a wide range of metallic utilities such as underground storage tanks, vault covers, wells, and other isolated metallic utilities buried up to 16.4 ft deep (ASCE 2002). Under some conditions, the technique can be used as well to detect large, nonmetallic utilities such as water pipes in dry soils and empty and dry pipes in wet soils (ASCE 2002). The performance of terrain conductivity imaging can be affected considerably by interfering magnetic fields noise produced along overhead power lines and aboveground metal objects, such as vehicles, fences, or buildings (Jeong and Abraham 2004), and by the physical and chemical properties of the surrounding soils. The conductivity of a soil depends significantly on the size of its particles: the smaller the particles are in the surrounding soil, the higher the conductivity is since fine-grained soils transmit the EM currents in easier and more direct wave paths. In the previous SHRP 2 study (Young and Kennedy 2015), TDEM, the complementary approach to FDEM, was evaluated as part of a vehicle-mounted system where a novel multitransmitter instrument was deployed. The present study sought to evaluate the capabilities of FDEM because this method has the potential to determine the depth of a buried utility as a function of the frequency at which the utility is detected.

## MAGNETIC METHODS

The Earth behaves like a large magnet, and its magnetic field is typically represented with lines much like it is for a common magnet. So, at every point on and below the surface of the Earth, there is a level of magnetic field present. Objects made of certain materials, such as iron, steel, and ferromagnetic alloys, are affected by this field in such a way that they develop their own magnetic field very similar to that of a magnet. By contrast, buried objects made of nonmagnetic metals, such as aluminum, copper, and gold, are not affected by the Earth's magnetic field and therefore cannot be detected by magnetic locators.

The most basic magnetic field sensor is a search coil or antenna, which consists of a coil of wire wrapped around ferrite rods. When an alternating magnetic field cuts through the search coil, a voltage proportional to the strength of the magnetic field is produced. Generally, search coils are arranged in triplet clusters, one for each of the Cartesian axes. In this way, a three-dimensional (3D) vector of the magnetic field can be generated for any point in space.

### Magnetic Locators

Magnetic locators operate on the principle of detecting the difference in the magnetic field present at two sensors spaced a fixed distance apart. In the absence of a buried object, the field at both sensors is the same. The presence of an object made of iron or steel results in a difference between the magnetic field at the top and the bottom sensors. That difference is called a gradient. Magnetic locators indicate the detection of a gradient by changing the pitch of an audio tone and, depending on the model, with a bar graph on a visual display. The size of the buried object has an impact on the size of the magnetic field difference or gradient. Likewise, the orientation of the buried object also affects the size of the gradient detected. The same object oriented vertically will generally produce a larger difference. Some locators also indicate polarity, which can be

useful in determining whether the target is oriented vertically or horizontally. This is accomplished by observing the polarity change at each end. The fixed spacing between the sensors determines the overall length of a locator. It has an impact on the field difference detected or the sensitivity of the locator. The farther apart the sensors are, the more sensitive the locator becomes.

### Magnetometers

Ferrous metal or magnetic locators, commonly referred to as magnetometers, have long been employed by both geophysicists and archaeologists for detecting underground objects and rock formations. They detect variations in the Earth's magnetic field as a result of underground features such as metallic pipes, underground storage tanks, or ore bodies. Consequently, only objects containing iron can be detected, thereby greatly limiting its value as a general technique for locating and identifying buried pipelines. The quality of results can also be affected by nearby buildings, cables, fences, and other metallic objects (Vickridge and Leontidis 1997), and it is, therefore, a technique that should be used with care and in conjunction with other devices.

Several types of magnetometers are in use, but the most common are the fluxgate magnetometers and the proton precession magnetometers. The fluxgate magnetometer is a device that measures the intensity and orientation of magnetic lines of flux in three orthogonal directions (Telford, Geldart, and Sheriff 1990). Fluxgate magnetometers have been used in many applications, such as geological prospecting, underground detection, aerospace navigation, underwater navigation, land navigation, and submarine detection. The heart of the fluxgate magnetometer is a ferromagnetic core surrounded by two coils of wire in a configuration resembling a transformer. AC is passed through one coil, called the primary, producing an alternating magnetic field that induces AC in the other coil, called the secondary. The intensity and phase of the AC in the secondary are constantly measured. When a change occurs in the external magnetic field, the output of the secondary coil changes. The extent and phase of this change can be analyzed to determine the intensity and orientation of the flux lines.

The proton precession magnetometer is the most commonly used instrument for measuring the Earth's magnetic field (Talwani and Kessinger 2003). In its simplest form, the instrument consists of a bottle filled with water. A strong electric current is passed for a few seconds through a coil wound around the bottle. Water is a paramagnetic substance and can be thought of as containing an assemblage of tiny magnets that execute random, thermally induced motions. When the current is turned off, the coil is used to record the current now produced by the tiny magnets as they process around the direction of the Earth's ambient magnetic field. The frequency of precession is proportional to the Earth's field and is conveniently recorded by digital counters, and thus the value of the magnetic field can be obtained.

## SEISMIC AND ACOUSTIC METHODS

Acoustic and seismic methods to detect underground utilities are especially useful in situations when GPR and EM fail due to soil properties, conductivity issues, or electrical noise (Miller et al. 2000). These common obstacles seen with EM methods have no effect on the generation of acoustic and seismic waves. Additionally, EM methods depend on a discrepancy in the conductivity or permittivity between the buried pipes and the surrounding medium, which makes

EM unusable for some targets, such as plastic, water-filled pipes (Papandreou, Rustighi, and Brennan 2008). The following sections review NDE methods that use seismic and/or acoustic waves to interrogate the subsurface; describe their use, advantages, and limitations; and recommend promising methods for further investigation.

## Traditional Acoustic Methods

Research to understand the behavior of acoustic waves in buried pipelines is extensive. Acoustic-wave methods divide into two types depending on whether there is direct access to a pipeline. Multiple acoustic techniques rely on access to a pipeline, e.g., a hydrant or manhole, to attach an acoustic source. With access to the pipe, there are three main ways to generate acoustic waves: active sonics, which measures sound waves in a pipe caused by striking it at an exposed point, passive sonics, which measures the vibrations associated with leaks escaping from pressurized buried pipes, and resonant sonics, which depends on the contents of the pipe being a noncompressible fluid and generating a pressure wave in the fluid to detect pipe vibrations (Jeong and Abraham 2004).

A traditional acoustic transmission method, an acoustic pipe locator (APL), requires an acoustic generator and, typically, a single receiver in the form of a geophone or headphones. The concept behind the method is regions with more intense signals correlate better to the buried pipe locations. Liu et al. (2020) determined that a frequency range from 50 to 150 Hz is most effective for pipe detection, although it is dependent on soil type. Detection results are prone to interference from noise and distortion from surrounding medium properties, and interpretation of the results relies heavily on the user (Sterling et al. 2009).

## Seismic Methods

Similar to acoustic technologies, seismic waves remain unaffected by wet soil conditions and conductivity issues. Specifically, analyzing seismic surface waves is advantageous because they are relatively large in amplitude, which can provide ideal signal-to-noise ratios in areas with elevated levels of mechanical or acoustic noise. During the SHRP 2 study, the use of a prototype seismic shear wave reflection imaging system was demonstrated, which is field and data processing intensive (Young and Kennedy 2015). For this effort, the benefits and disadvantages of three seismic surface-wave methods were demonstrated: spectral analysis of surface waves (SASW), MASW, and horizontal-to-vertical spectral ratio (HVSR). One or a combination of these methods may be useful in various situations to support EM recordings or used in substitution when EM technologies are not effective (e.g., loose soil, nonconductive materials, or physical obstacles).

### *SASW*

SASW leverages the dispersive characteristic of Rayleigh waves in an inhomogeneous medium (Fernández, Hermanns et al. 2011). As an active source method, surface waves are generated by dynamic sources, such as hammers, weight drops, vibroseis, and bulldozers, at a variety of frequencies. SASW is ideal for measuring shear wave velocity with depth through inversion of dispersion curves (Badsar et al. 2010). This method can be applied to both bare and paved surfaces, is ideal for depths up to 147.6 ft, and is not limited by soil type.

Minimum requirements for SASW are two receivers (geophones or accelerometers) at known offsets and one source. Accelerometers are useful for high-frequency studies at shallow depths on stiff surfaces like pavement, and geophones are ideal for lower frequency studies deeper in soils (Al-Shayea, Woods, and Gilmore 1994). The accessible area on the surface needs to be equal to or greater than the depth required, which is an easy requirement for shallow-buried utilities (GEOVision 2016). Multiple dispersive layers indicate the presence of stiffer materials that may coincide with buried objects.

### *MASW*

Conventional SASW is limited by multiple factors, including phase unwrapping errors, inefficient data filtering, and failure to classify multiple modes (Lin, Lin, and Chien 2017). Unlike the two-channel SASW method, MASW implements a two-dimensional (2D) wavefield transformation to produce images of subsurface shear-wave velocity (Park, Miller, and Xia 1996; Xia et al. 1998; Park, Miller, and Xia 1999; Xia, Miller, and Park 1999; Lin, Lin, and Chien 2017). Utilizing surface-wave energy between 1 and 30 Hz on multiple channels (minimum of 24 geophones), MASW generates surface waves using an active (sledgehammer) or passive (traffic, tidal motions, thunder) source (Park et al. 2007). For shallower studies, an active source is ideal as it images objects at depths less than 98.4 ft.

By exploiting the dispersion of surface waves through pits, trenches, or buried utilities compared to the surrounding medium, MASW software can locate localized zones of subsurface anomalies, including pipes. As an example, one utility software package generates a shear velocity ($V_s$) profile through dispersion-curve analysis from a multichannel record and then an inversion process (Park et al. 2000). Miller et al. (2000) combined MASW with a common middle point data acquisition to delineate vertical and horizontal variations in subsurface materials.

### *HVSR*

HVSR may be performed in conjunction with MASW as a straightforward, passive seismic method for subsurface mapping (Mendecki, Bieta, and Mycka 2014; Sauret et al. 2015). Khalil, Anukwu, and Nordin (2020) successfully applied the HVSR technique to mapping underground utilities by exploiting the higher velocities in utilities compared to that of the soil. This discrepancy generates an impedance contrast between the utility and the subsurface layers because their densities and velocities differ. HVSR methodology is commonly used in the United States for soil resonance and site response studies, but there are no available case studies of the technique applied to underground utilities. Given the success of Khalil, Anukwu, and Nordin (2020) in Malaysia, their methodology could be applied to buried pipe and utilities detection in the United States. Figure 4 shows the pseudo 3D HVSR section they generated from multiple geophones. The depth (z-axis) was obtained by converting from the frequency domain to the depth domain. Dashed and solid lines represent the trend of possible subsurface utilities.

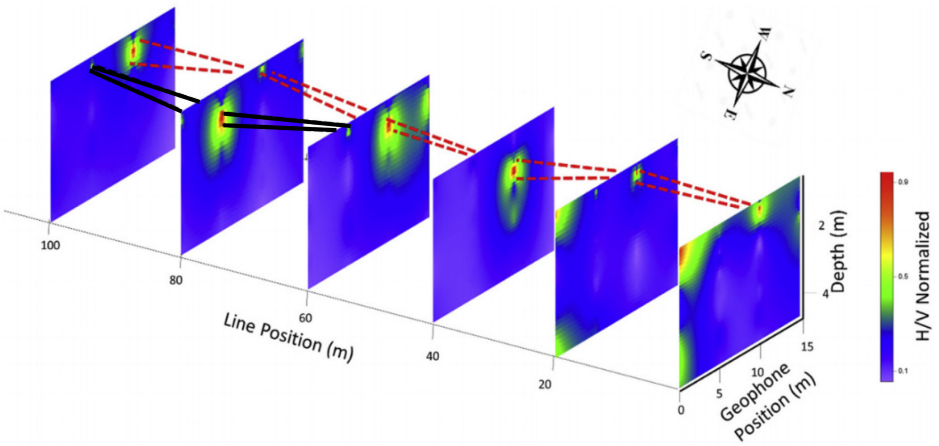




**Figure 4. Image. Pseudo 3D HVSR section generated from multiple geophones (Khalil, Anukwu, and Nordin 2020).**

## SUMMARY

Table 1 presents a summary of the key advantages, limitations, and other technical details surrounding the technologies reviewed in this section.

**Table 1. Summary of researched NDE technologies.**

| NDE Technology | Advantages | Limitations | Automation Capabilities | Other Issues |
|---|---|---|---|---|
| **GPR technologies** | • Most utility types detected (including plastic, nonmetallic, and metal).<br>• Wide market availability and efficient power usage.<br>• Highest available spatial resolution under favorable conditions. | • Highly sensitive to soil type and utility electrical conductivity.<br>• Signal scatters in heterogeneous subsurface conditions.<br>• Suffers in presence of nearby conductive materials. | • Automated data acquisition and processing available.<br>• High-quality image visualizations in 3D. | • Requires significant analyst training for accurate feature interpretation. |
| **Magnetic locator technology** | • Measures intensity of buried ferromagnetic materials (manmade objects containing iron or steel).<br>• Detects underground storage tanks and buried manhole covers.<br>• Detects buried military ordnance. | • Sensitive to environmental factors (induced magnetic fields).<br>• Limited bandwidth.<br>• Sensitive to interference. | • Automated features available (gain, depth readings, etc.). | • Fields induced in reinforcements in pavement above utility destroy detection capabilities. |
| **EM technologies:**<br>**Pipe and cable locators** | • Detects buried copper, aluminum, and steel objects.<br>• Precise location capabilities even in the presence of signal distortion.<br>• Already widely used in subsurface utility tracking. | • Sensitive to cable and pipe diameters and types.<br>• Sensitive to soil conditions.<br>• Performance degrades in proximity to nearby conductors. | • Automated features available (gain, depth readings, etc.). | • Field distortion (asymmetrical EM fields) can occur in complicated, multiconductor underground topologies. |

| NDE Technology | Advantages | Limitations | Automation Capabilities | Other Issues |
|---|---|---|---|---|
| **EM technologies:**<br>**Terrain conductivity method** | • Detects wide range of utilities.<br>• Moderately inexpensive.<br>• Useful in areas with nonutility congestion or high ambient conductivity. | • Moderate-to-poor accuracy.<br>• Sensitive to instrument and subsurface noise.<br>• Subject to unexpected spikes (extreme conductivity values).<br>• Sensitive to wave attenuation. | • Automated data acquisition, conditioning, and processing available. | • Fields induced in reinforcements in pavement above utility destroy detection capabilities. |
| **Acoustic technologies:**<br>**APL** | • Identifies metal, PVC, concrete, and clay underground targets. Not limited by pipe conductivity or soft soil.<br>• Ideal for shallow targets (12–96 inches below surface). | • Detection and approximate locations only.<br>• Minimum target size of 0.5 inches required; poor depth resolution. | • Real-time data visualization available. | • Underdeveloped for the utility detection and location application. |
| **Seismic technologies:**<br>**MASW** | • Not limited by pipe conductivity or soft soil. Identifies plastic and metal targets under grass and pavement.<br>• Ideal for shallow targets (12–96 inches below surface). | • Moderate depth precision (+/- 15 percent).<br>• Requires slower data acquisition and multigeophone array. | • Multiple data-processing software packages available. | • Data-processing improvements still needed prior to commercial implementation. |
| **Seismic technologies:**<br>**HVSR** | • Not limited by pipe conductivity or soft soil. Identifies plastic and metal targets under grass and pavement.<br>• Ideal for shallow targets (12–96 inches below surface). | • Moderate depth precision (+/- 10 percent).<br>• Requires three-component geophones. | • None. | • Less well developed and tested than other NDE techniques for utility detection and location.<br>• Could be performed concurrently with MASW to improve outcomes. |

PVC = polyvinyl chloride.

# CHAPTER 3. STATE DOT IMPLEMENTATION

Two key objectives of this study were to understand how State DOTs currently use NDE technologies to detect and locate buried utilities and to recommend emerging techniques that merit implementation. The implementation assistance program that followed the SHRP 2 R06D study allowed multiple States to use NDE technologies. FHWA requested an update on the extent to which State DOTs have used these technologies successfully to identify underground utilities in both existing and new construction.

To determine the current usage of NDE technologies, the project team performed a limited survey (polling) of nine State DOTs (California, Florida, Kentucky, Louisiana, Minnesota, Missouri, Oregon, Texas, and Virginia) to document their practices and concerns and to determine whether they used in-house or hired services for underground utility location, the types of technologies they typically used, and the advantages and limitations of those use cases. All results are available on request. Figure 5, figure 6, figure 7, figure 8, and figure 9 present summarized results of the survey.

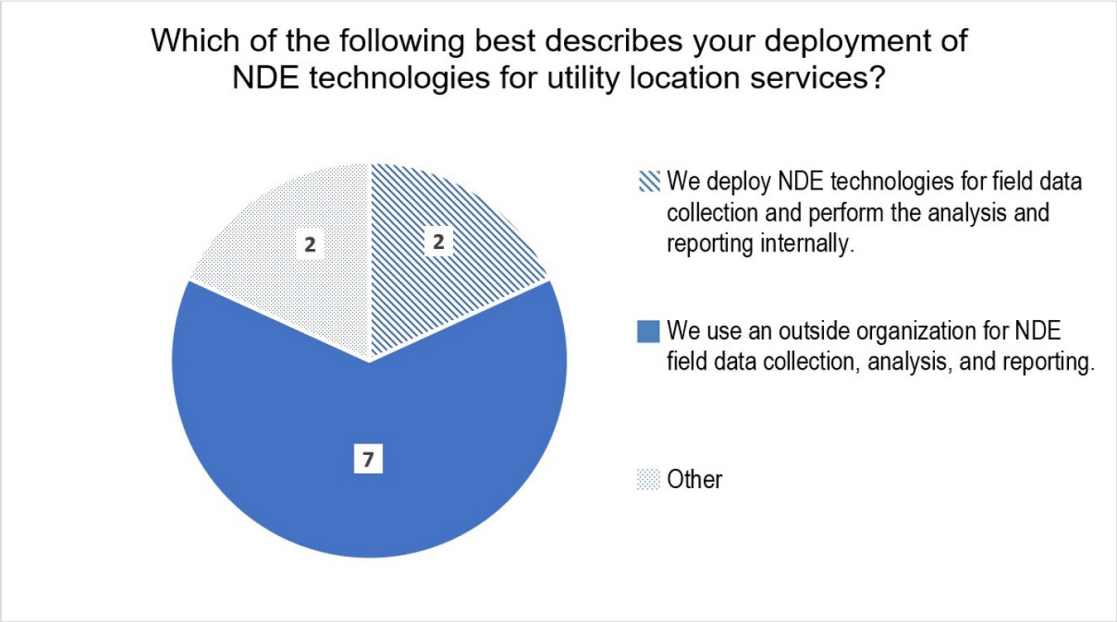


Source: FHWA.

**Figure 5. Chart. Survey response from DOTs regarding internal and external use of NDE technologies.**

In figure 5, the striped pattern represents "We deploy NDE technologies for field data collection and perform the analysis and reporting internally." The dotted pattern represents "We deploy NDE technologies for field data collection and use an outside organization for analysis and reporting." The solid pattern represents "We use an outside organization for NDE field data collection, analysis, and reporting."

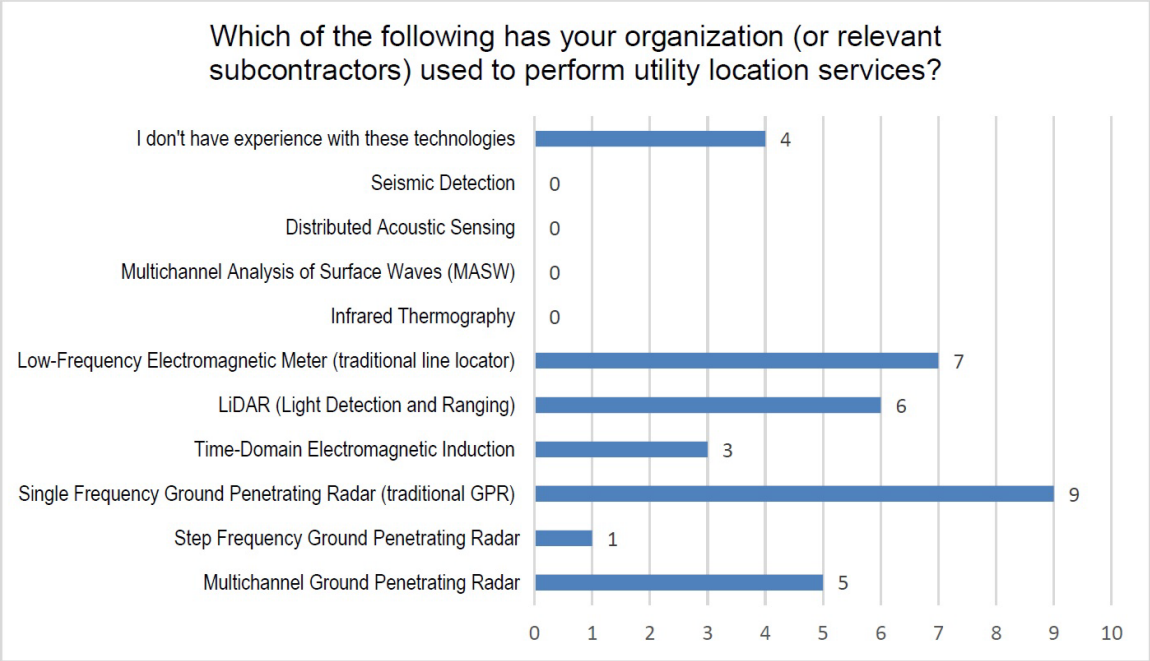


Source: FHWA.

**Figure 6. Graph. Survey response regarding types of NDE technologies used.**

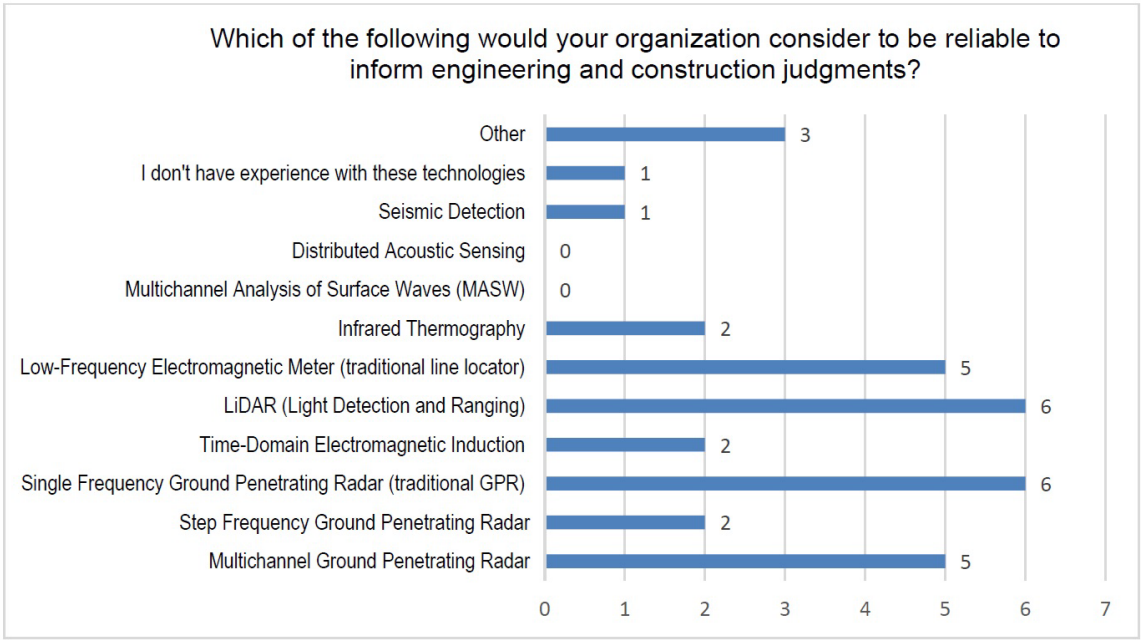


Source: FHWA.

**Figure 7. Graph. Survey response on which types of NDE technologies are reliable to inform engineering and construction judgments.**

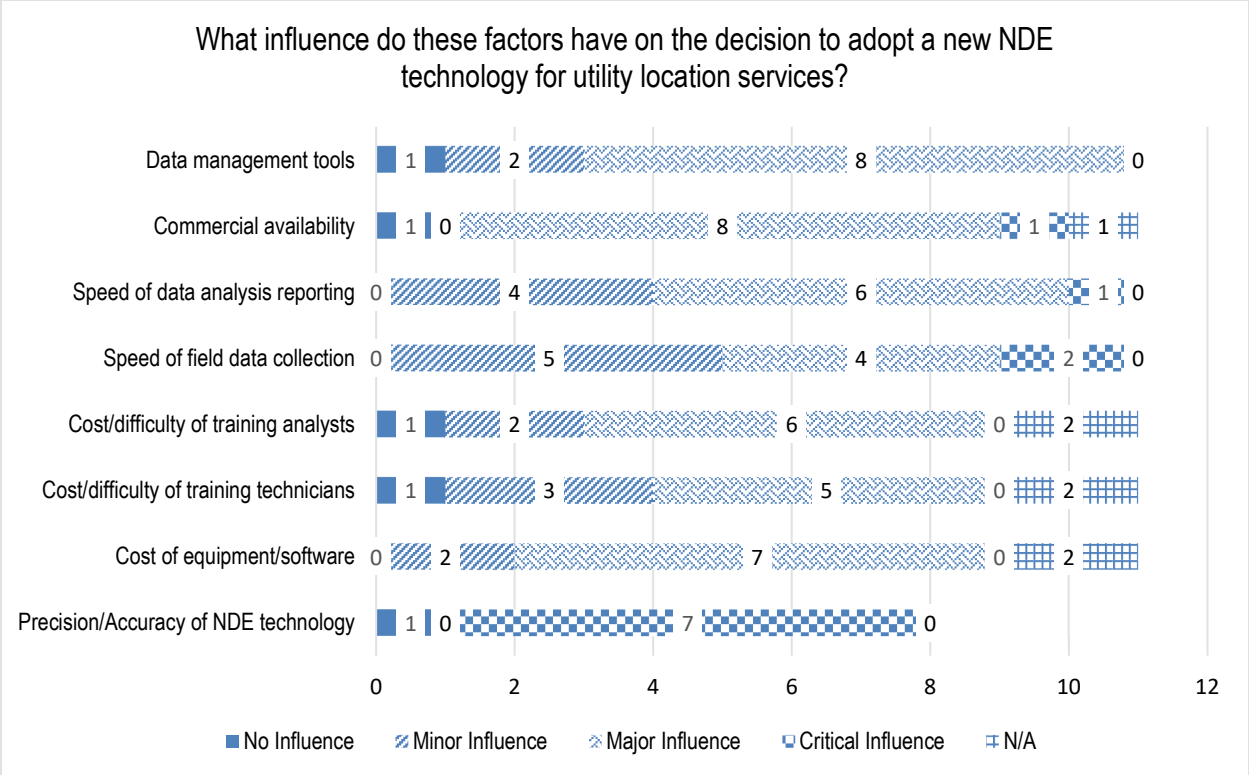


Source: FHWA.

**Figure 8. Graph. Survey response on influence factors on adopting new NDE technologies for utility location.**

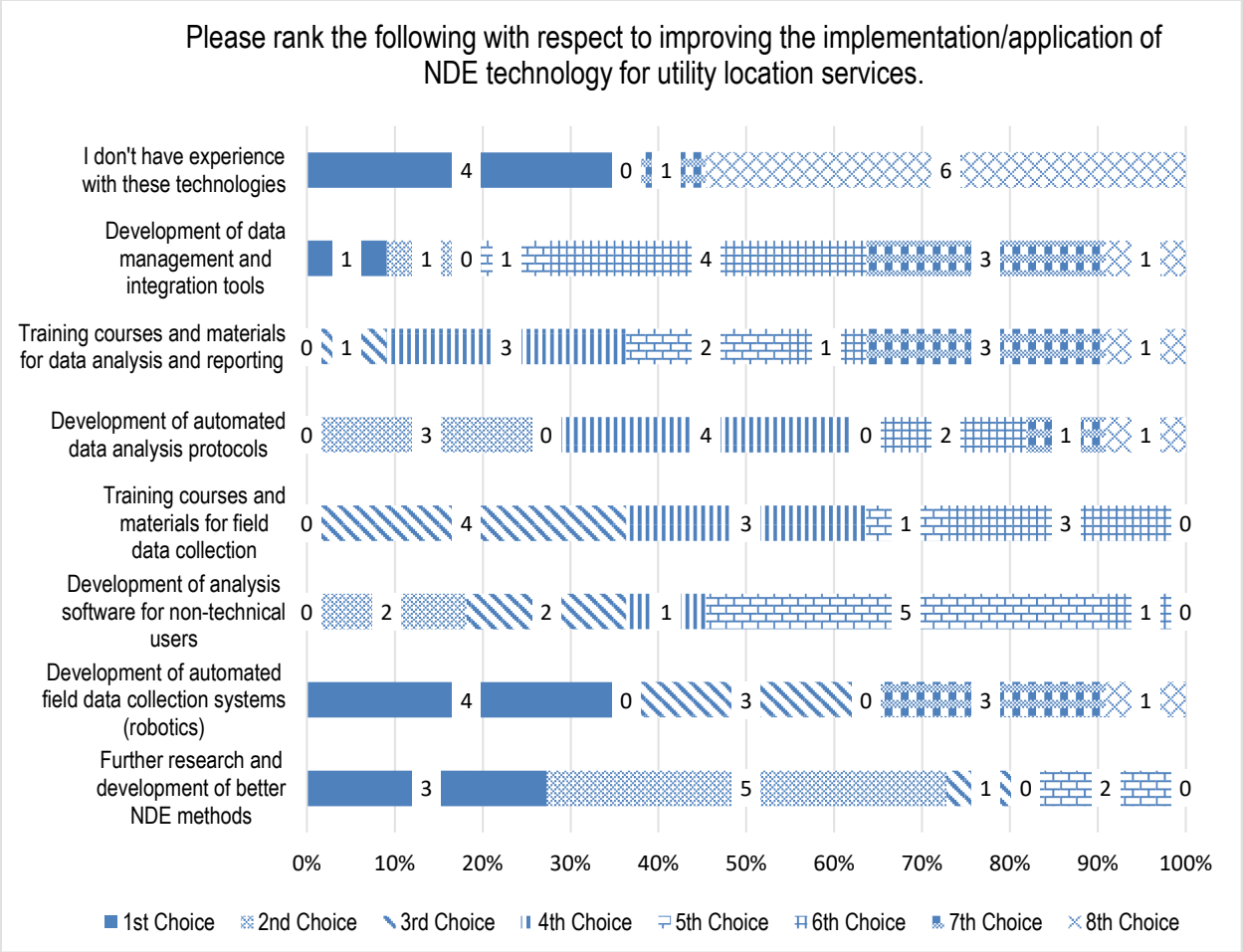


Source: FHWA.

**Figure 9. Graph. Survey response regarding the ranking of improvements needed for the implementation and/or application of NDE technologies for utility location services.**

Surveys of staff members in nine DOT offices revealed several points: GPR is the most commonly used technique for utility detection, followed by traditional magnetic line locators and TDEM induction. Seismic and acoustic techniques are underutilized to detect buried utilities. High interest exists in automating data collection and data processing. More guidance on best practices in various environments would be used by DOTs, and accurate location readings from NDE technologies are the most important aspect to DOT personnel.

The State DOT survey responses helped prioritize the lab and field experiments. The project team had not considered TDEM/FDEM methods in the early study; however, based on feedback and interest from DOT personnel and FHWA, the field tests included FDEM. The NDE technologies selected for lab and field experiments included GPR, TDEM/FDEM, MASW/HVSR, and APL methods. All methods have strong imaging capabilities at shallow depths, do not require access to a pipeline, and can be used in conjunction with one another to improve outcomes and decrease uncertainty. Additionally, most of the data-collection hardware and protocols for the selected methods were already available in the commercial market.

# CHAPTER 4. CONTROLLED LAB AND FIELD EXPERIMENTS

While the literature search and industry review yielded important findings on the state and availability of modern NDE technologies for locating buried utilities, the next important step in this study was evaluating these technologies side-by-side to determine their efficacy in equal test conditions. GPR, FDEM, MASW, HVSR, and APL were the methods selected for evaluation during this part of the project. They were chosen for their ability to be used on grade without the need for utility exposure, their relevant equipment and systems being readily available in the market for use, and the existence of established procedures and processes for their deployment. The point on availability was particularly important here as many of the techniques reviewed in the literature were demonstrated to be viable in theory but are not ready for testing in practice such that State DOTs would ultimately be able to deploy them if they are found to be effective in utility location.

The project team developed a laboratory testing plan to thoroughly evaluate the different selected NDE technologies. A matrix of specimens was designed and tested, for which typical utility pipes of varying sizes were buried in different soil conditions and burial configurations to assess the effectiveness of each NDE technology in a controlled setting. A combination of soil-filled enclosures was designed, built, and tested under different controlled configurations. Four specimen types were investigated: fine-grained cohesive soil, coarse-grained cohesionless soil, two layers of cohesive soils at the bottom and cohesionless soil on top, and two layers of cohesionless soil at the bottom and cohesive soil on top.

The laboratory specimens were designed and built at a North Carolina DOT indoor facility. The specimens consisted of soil-filled enclosures made of raised garden beds stacked on top of each other. Each raised bed consisted of a wooden frame measuring 12 ft × 5 ft × 1 ft, with a total of six beds being added incrementally as scans were completed over the embedded utility pipes. The incremental addition of each bed was referred to as a lift. Figure 10, figure 11, figure 12, and figure 13 present diagrams of the stacked beds for the cohesive soil, cohesionless soil, and mixed soil type of specimens, while figure 14 presents an image of the specimens under construction.

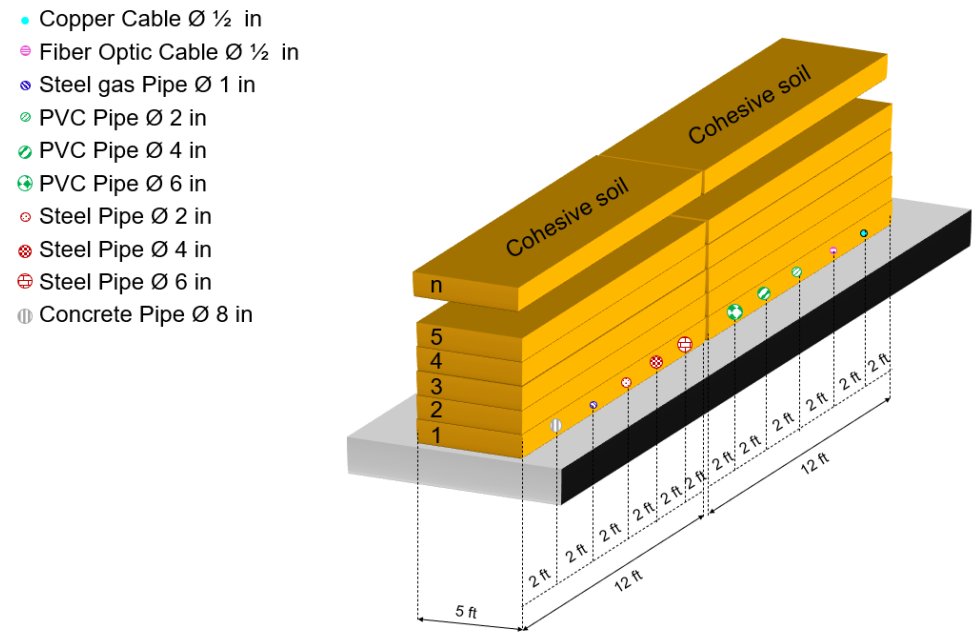


Source: FHWA.

**Figure 10. Illustration. Soil box specimen with six total beds of cohesive soil stacked together.**

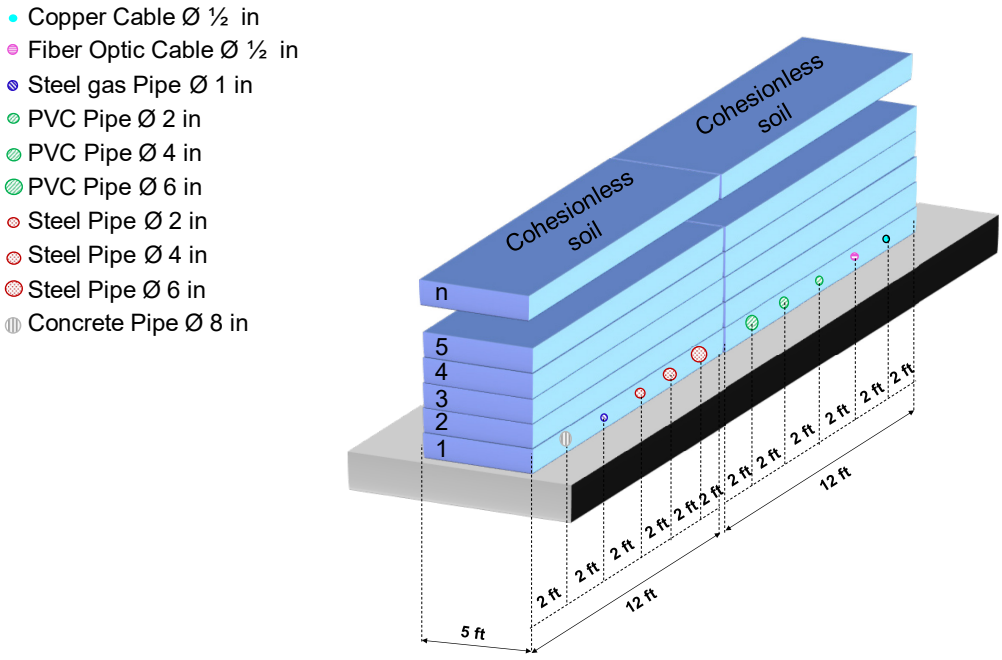


Source: FHWA.

**Figure 11. Illustration. Soil box specimen with six total beds of cohesionless soil stacked together.**

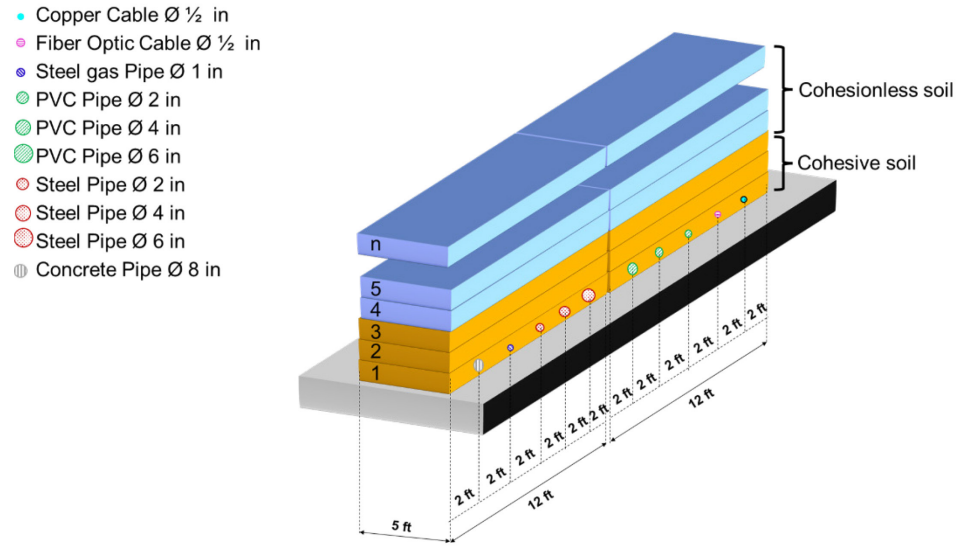


Source: FHWA.

**Figure 12. Illustration. Soil box specimen with six total beds of cohesive and cohesionless soil stacked together.**

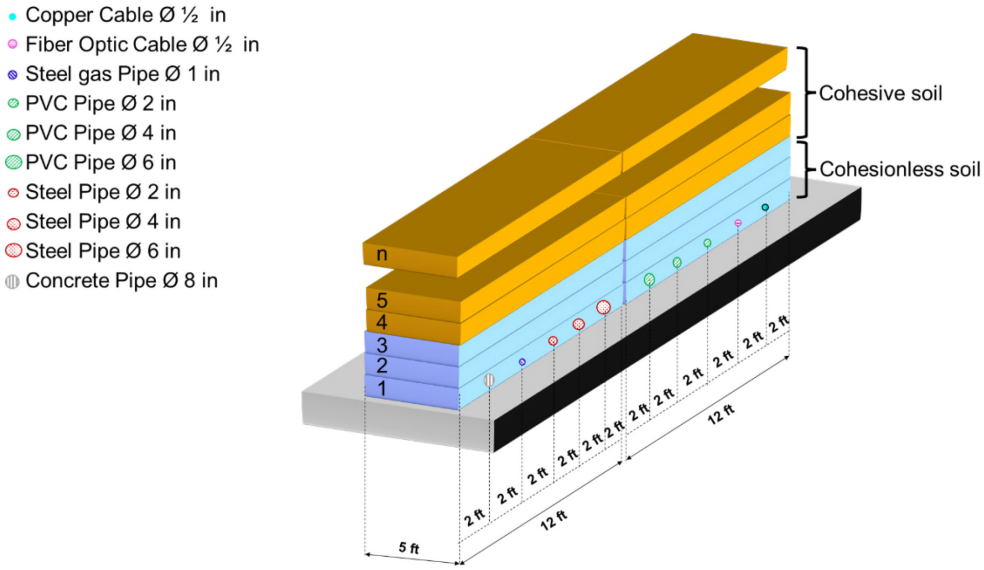


Source: FHWA.

**Figure 13. Illustration. Soil box specimen with six total beds of cohesionless and cohesive soil stacked together.**

Source: FHWA.

**Figure 14. Photo. First level of soil box specimens with buried utilities in parallel.**

## TEST METHODS AND INSTRUMENTATION

### Stepped-Frequency GPR Field Plan and Results

The GPR instrument used for field testing featured unique stepped-frequency, continuous-wave radar technology that provides a frequency range of 200–3,440 MHz. This range of frequencies means that the high-precision measurements associated with high-frequency signals can be captured at the same time as the high-penetration depth measurements associated with low-frequency signals. Scans were taken on each type of soil box at each lift level, with the instrument being pushed along the soil transverse to the orientation of the buried targets. Figure 15 presents an image of the GPR system in use on a given soil box.

Source: FHWA.

**Figure 15. Photo. GPR system with integrated cart scanning soil box.**

The scans gathered using the GPR were analyzed by reviewing them for the signature hyperbolic peaks that are produced by subsurface targets, as presented in figure 16, figure 17, figure 18, and figure 19. These peaks were tracked across each test lift for the four specimen types to identify the depth at which the feature was no longer visible. Table 2 summarizes these findings for each pipe and specimen type, respectively.

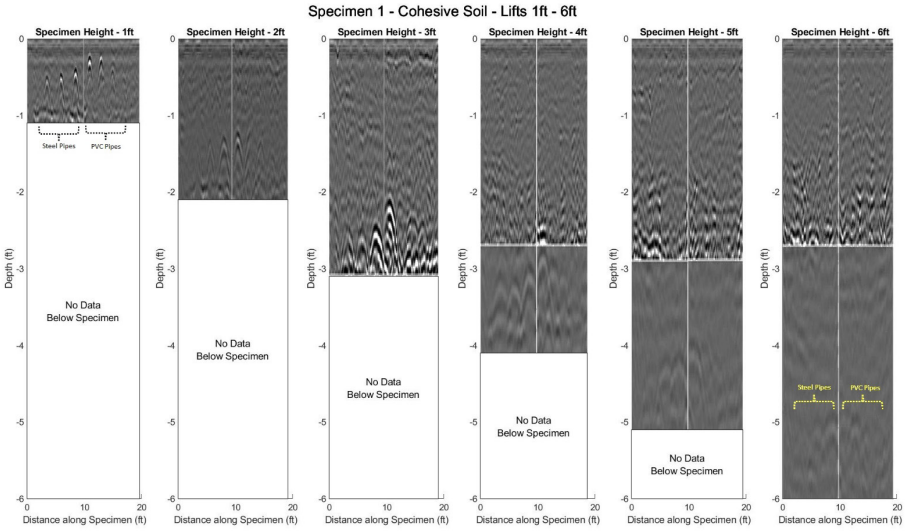


Source: FHWA.

**Figure 16. Image. GPR scans collected on cohesive soil test specimen, where each of the hyperbolic peaks represents a buried utility observed in the data.**

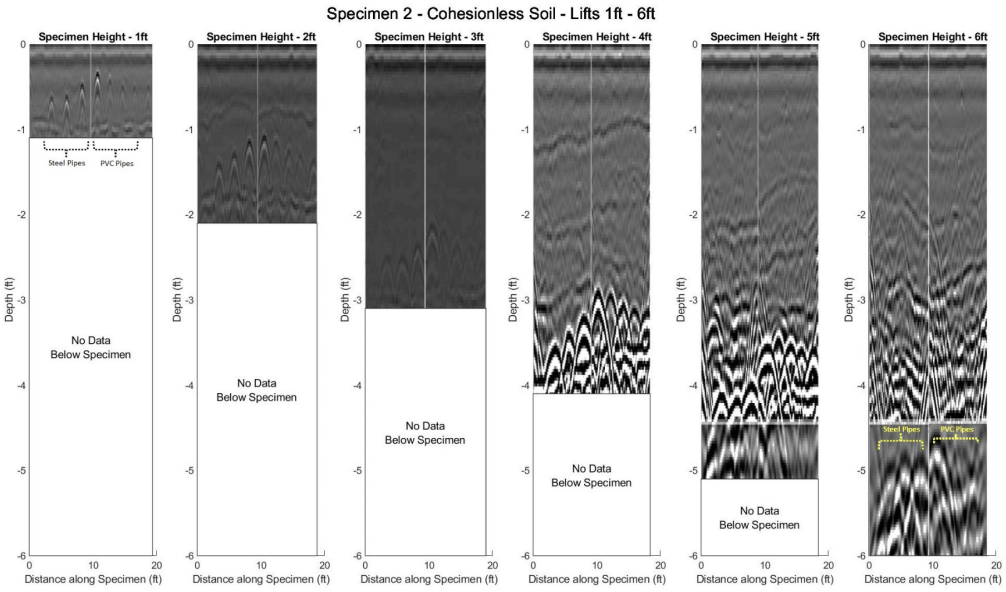


Source: FHWA.

**Figure 17. Image. GPR scans collected on cohesionless soil test specimen, where each of the hyperbolic peaks represents a buried utility observed in the data.**

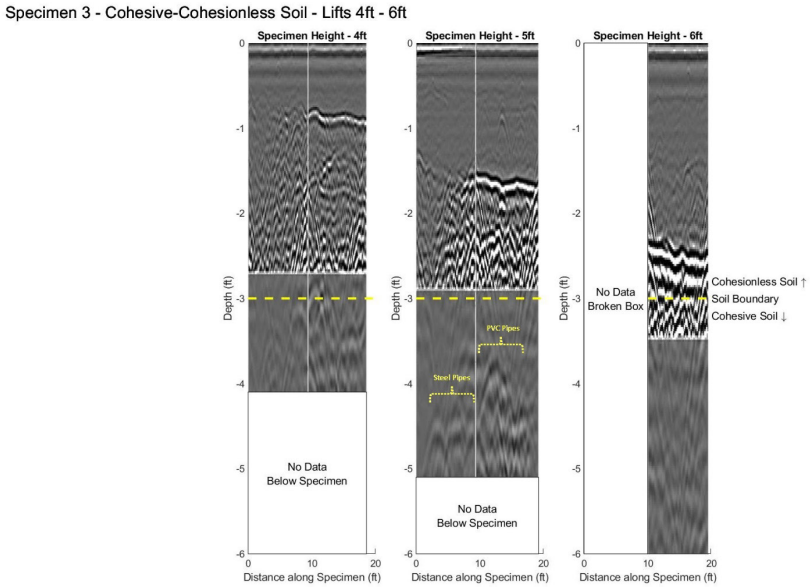


Source: FHWA.

**Figure 18. Image. GPR scans collected on cohesive-cohesionless soil test specimen, where each of the hyperbolic peaks represents a buried utility observed in the data.**

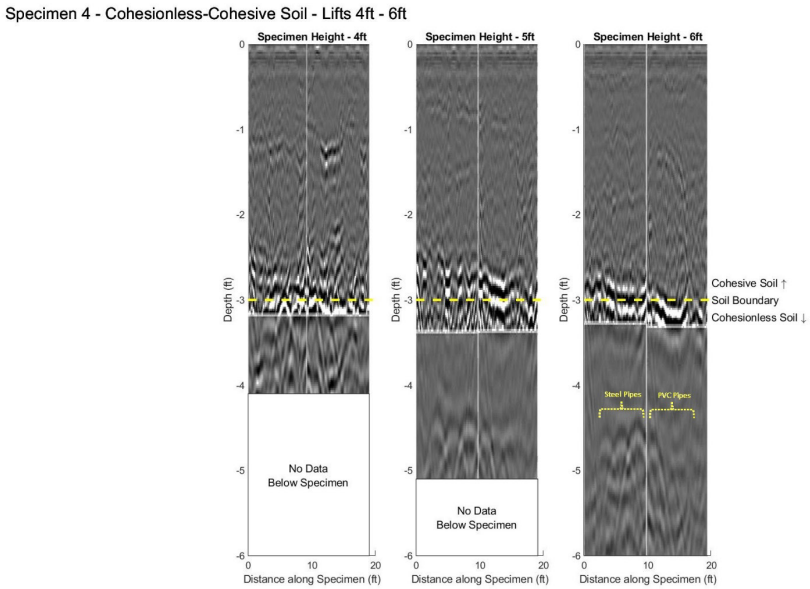


Source: FHWA.

**Figure 19. Image. GPR scans collected on cohesionless-cohesive soil test specimen, where each of the hyperbolic peaks represents a buried utility observed in the data.**

**Table 2. Summary of maximum observable lift allowing visualization of subsurface target with GPR.**

| Maximum Observable Lift | Specimen 1 | Specimen 2 | Specimen 3 | Specimen 4 |
|---|---|---|---|---|
| Concrete pipe | 0 | 0 | 0* | 0* |
| Fiber optic cable | 0 | 0 | 0* | 0* |
| 1-inch Copper pipe | 5 | 6 | 4* | 6* |
| 2-inch Steel pipe | 5 | 6 | 6* | 6* |
| 4-inch Steel pipe | 6 | 6 | 6* | 6* |
| 6-inch Steel pipe | 6 | 6 | 6* | 6* |
| 6-inch PVC pipe | 4 | 5 | 6* | 6* |
| 4-inch PVC pipe | 4 | 5 | 0* | 0* |
| 2-inch PVC pipe | 3 | 5 | 0* | 0* |
| Insulated copper wire | 2 | 5 | 0* | 0* |

*Tests only completed for top lifts 4–6.

## Pipe and Cable Locators Field Plan and Results

The project team used an underground utilities locator instrument to perform pipe and cable locations. The system allows for the use of a passive detection mode and an active detection mode where a signal can be injected into a given conductive material to track its position underground. Scanning with the instrument was performed manually, with a systematic approach being taken to cover the entire soil box and detect the subsurface targets according to the instructions in the instrument documentation. This instrument was used on every box and at every lift under investigation. An image of it in operation is shown in figure 20.

In passive operation mode, the instrument was unable to locate any of the subsurface targets using the advised method for its deployment. This failure included the steel and copper pipes that were made of conductive materials. As a check on the equipment, the instrument was also operated in its active mode, where a signal was injected into the conductive pipes to detect the target's presence. This operation approach was successful for the copper pipe and every size of the steel pipes to lift level 6 for each specimen.

Source: FHWA.

**Figure 20. Photo. Underground utilities locator scanning over steel pipe.**

### APL Field Plan and Results

The largest uncertainty with an APL is the presence of inhomogeneous soil, including air pockets; however, under the controlled experiment setup, the field team was able to reduce this cause of error by compacting the soil through manual tamping. Data collection was performed at an interval of every 6 inches along the length of the soil boxes, with the instrument being operated in parallel with the orientation of the subsurface targets. Figure 21 presents an image of the APL in use.

Analysis of the APL data involved a review of the acoustic response B-scans gathered during testing to identify the presence of any clear peaks. While peaks were identified in some scans across the specimens and lifts, they generally did not align with the known lateral position of the subsurface targets, giving inconclusive results. It is possible that the limiting boundary conditions of the test specimens were ultimately not conducive to this test method, which is typically used in unbounded conditions.

Source: FHWA.

**Figure 21. Photo. APL in operation.**

### FDEM Instrument Field Plan and Results

The project team used a ground conductivity meter for FDEM measurements. Based on the documentation, the system was calibrated and nulled each day before testing. Data collection was performed at an interval of every 6 inches along the length of the soil boxes, with the instrument being operated in parallel with the orientation of the subsurface targets (figure 22). Analysis of the FDEM data involved a review of the collected relative conductivity values, looking for significant local minimums that typically indicate the presence of a conductive pipe. Figure 23 presents an example of an FDEM scan where two steel pipes are indicated by the two significant negative peaks in the data. Table 3 summarizes the results of this test method.

Source: FHWA.

**Figure 22. Photo. Ground conductivity meter in operation.**

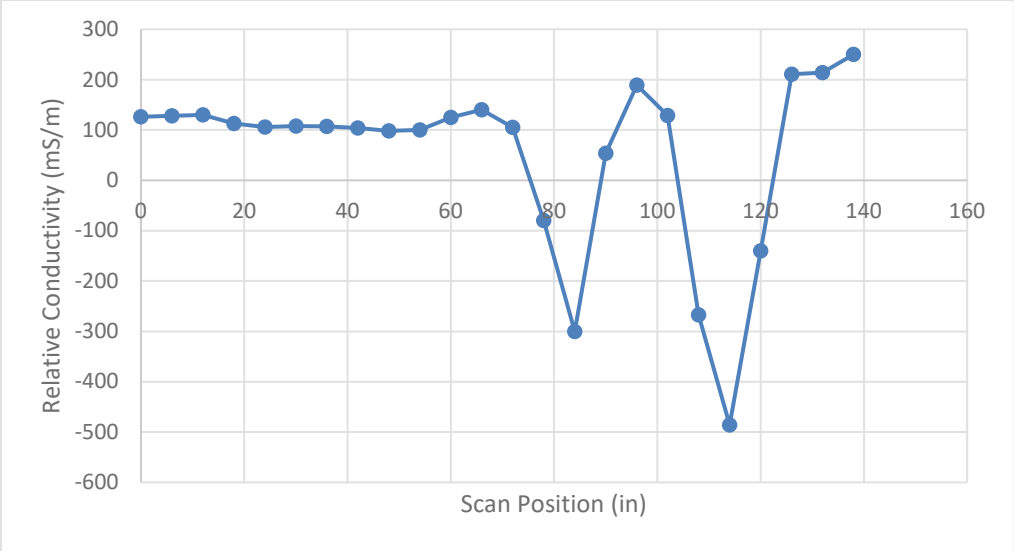


Source: FHWA.

**Figure 23. Graph. Example of FDEM scan with two steel pipes indicated by local minimums.**

**Table 3. Summary of maximum observable lift allowing visualization of subsurface target with FDEM.**

| Maximum Observable Lift | Specimen 1 | Specimen 2 | Specimen 3 | Specimen 4 |
|---|---|---|---|---|
| Concrete pipe | 0 | 0 | 0* | 0* |
| Fiber optic cable | 0 | 0 | 0* | 0* |
| 1-inch Copper pipe | 0 | 0 | 0* | 0* |
| 2-inch Steel pipe | 2 | 2 | 0* | 0* |
| 4-inch Steel pipe | 2 | 2 | 0* | 0* |
| 6-inch Steel pipe | 2 | 2 | 0* | 0* |
| 6-inch PVC pipe | 0 | 0 | 0* | 0* |
| 4-inch PVC pipe | 0 | 0 | 0* | 0* |
| 2-inch PVC pipe | 0 | 0 | 0* | 0* |
| Insulated copper wire | 0 | 0 | 0* | 0* |

*Tests only completed for lifts 4–6.

### HVSR Field Plan and Results

Using four broadband seismometers, the project team measured ambient noise for a 30-min duration across at least two transects running perpendicular to the pipes for box 1, box 2, and box 3 on one to two different lifts. The sensors were spaced so that every other sensor would be directly above a pipe (figure 24). The team was mainly interested in measurements on the two homogenous boxes because of the time-consuming nature of the test and because soil composition is less likely to have an effect on HVSR analysis; however, they also ran two 30-min tests on the mixed soil box, box 3. They also conducted two calibration tests on the ground near the test site to calculate the site frequency.

Source: FHWA.

**Figure 24. Photo. HVSR four-sensor test setup for soil box 1, lift 4.**

The team used the HVInv code (García-Jerez et al. 2016) to model ambient seismic energy and compute synthetic HVSR curves between 1 and 100 Hz in two models. The HVInv software relies on the diffuse field assumption, which specifies that the ambient seismic wavefield is composed of both shear and surface waves, unlike traditional HVSR methodology that assumes negligible surface waves (Nakamura 1989). This approach to HVSR processing is relatively straightforward, although different researchers use variations in the main methodology, which depends on the target depth, achievable resolution, study area, etc. The team followed the methodology of Khalil, Anukwu, and Nordin (2020) and Thompson et al. (2012) with a few adjustments due to the nature of the soil box and testing setup.

The soil box HVSR data were too inconsistent to confirm the presence of any pipes (see figure 25 for sample HVSR curves). The data inconsistency is likely related to the poor data-collection environment of the stacked testbed for ambient HVSR seismic measurements. The SESAME experiment (European Commission 2004) notes that HVSR measurements should be obtained in a quiet setting, with no anthropogenic noise (footsteps, machinery). Furthermore, the only available study of HVSR for nondestructive detection of underground utilities was carried out successfully in real-world conditions, not in a confined enclosure (the soil box walls) in close proximity to the pipes.

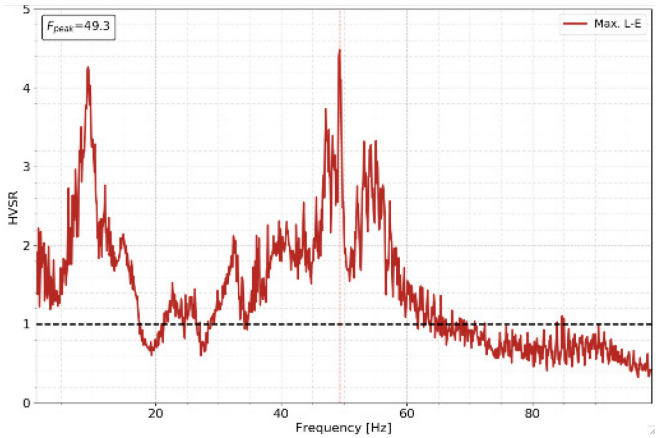


Source: FHWA.

A. HVSR plots for station 2 above the 6-ft steel pipe for box 1, lift 6.

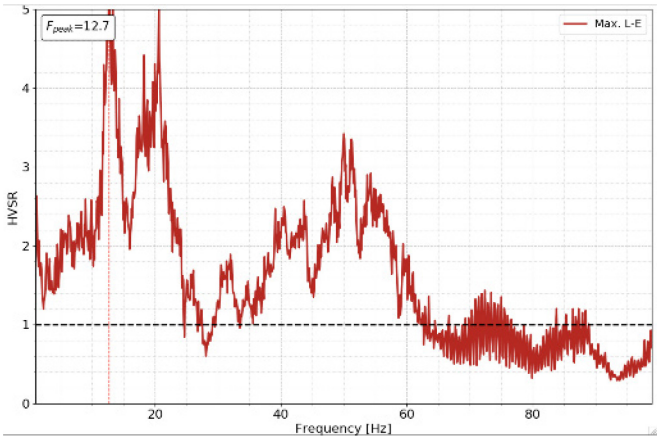


Source: FHWA.

B. HVSR plots for station 2 above the 6-ft steel pipe for box 1, lift 4.

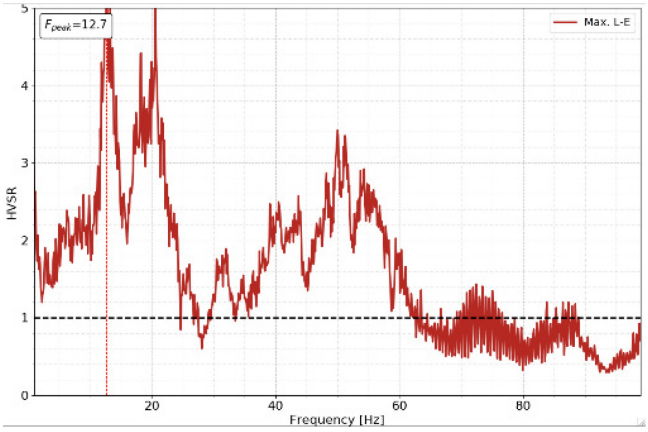


Source: FHWA.

C. HVSR plots for station 2 above the 6-ft steel pipe for box 2, lift 3.

**Figure 25. Graphs. HVSR plots to confirm the presence of any pipes.**

In figure 25, the six-layer model suggests that the peak due to the impedance contrast between the soil and steel should appear at approximately 32.5 Hz; however, the multiple frequency peaks observed across different boxes and lifts are too variable to confirm the success of the HVSR test in this experiment. Moreover, edge effects from the soil box are likely interfering with the results.

## CONTROLLED LABORATORY CONCLUSIONS

The laboratory testing phase of the study indicated that GPR was the most effective EM method capable of identifying buried utilities. FDEM exhibited a limited ability to detect utilities, and the passive-mode magnetic pipe locator produced no meaningful results. While a concrete pipe and fiber optic cable were not detected by any of the EM methods, GPR successfully found both polyvinyl chloride (PVC) and metallic targets down to depths of 4–6 ft. In contrast, the FDEM system successfully imaged larger metallic targets down to a depth of 2 ft. The homogeneous soil boxes presented fewer challenges to the EM technologies than the heterogeneous soil boxes.

The seismic and acoustic methods (MASW, HVSR, and APL, respectively) did not locate any buried utilities during the laboratory testing, primarily because the test conditions favored the EM techniques. The small soil boxes constructed for the laboratory testing introduced strong boundary effects, which created poor conditions for measuring clear seismic/acoustic wavefields. In addition, MASW/HVSR may have been confounded by the presence of high-frequency vibrational noise produced by equipment in the testing area. The project team determined that seismic and acoustic methods would be better suited to “boundary-free,” real-world conditions.

# CHAPTER 5. FIELD EXPERIMENTS—VIRGINIA DOT SITES

Based on the results from the controlled and laboratory experiments, the team field-tested a variety of NDE technologies in southern Virginia. Virginia DOT (VDOT) identified field sites with well-documented buried utilities and accessible locations for NDE technology tests. VDOT provided a list of possible field sites with buried utilities that varied in material type (PVC versus metal), diameter, and depth (shallow versus deep). The field team selected three VDOT-approved locations with similar sets of buried utilities, including PVC water and sewage pipes from 1 to 10 ft below the ground surface. The neighborhoods referred to throughout the report include Spring Hill (36.9323°N, -76.5898°E), Settlers Ridge (36.9391°N, -76.5060°E), and Windsong Way (36.9535°N, -76.5406°E); all three sites are located near the town of Carrollton, VA.

The team then evaluated the site locations and developed scan plans for the NDE tests after onsite walks and analyses of traffic conditions. Figure 26, figure 27, and figure 28 present the site maps for Spring Hill, Settlers Ridge, and Windsong Way, with their respective utility types and locations denoted.

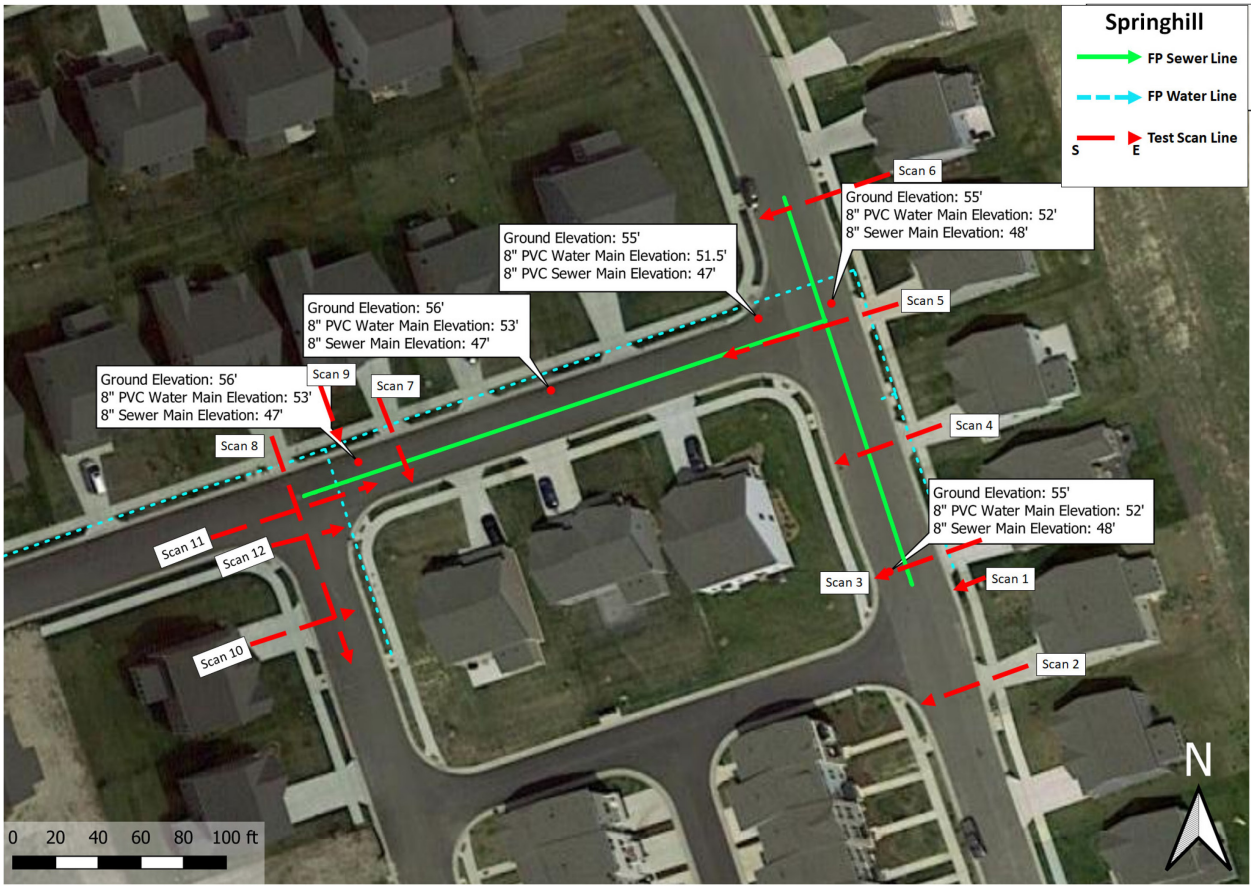


Original Photo: © 2021 Google® (see Acknowledgments section). Image modified by FHWA to identify utility types and locations.
FP = from plans.

**Figure 26. Photo. Aerial view of the Spring Hill field site with utility locations, elevations, and type indicated with solid (sewer) or dashed (water) lines.**

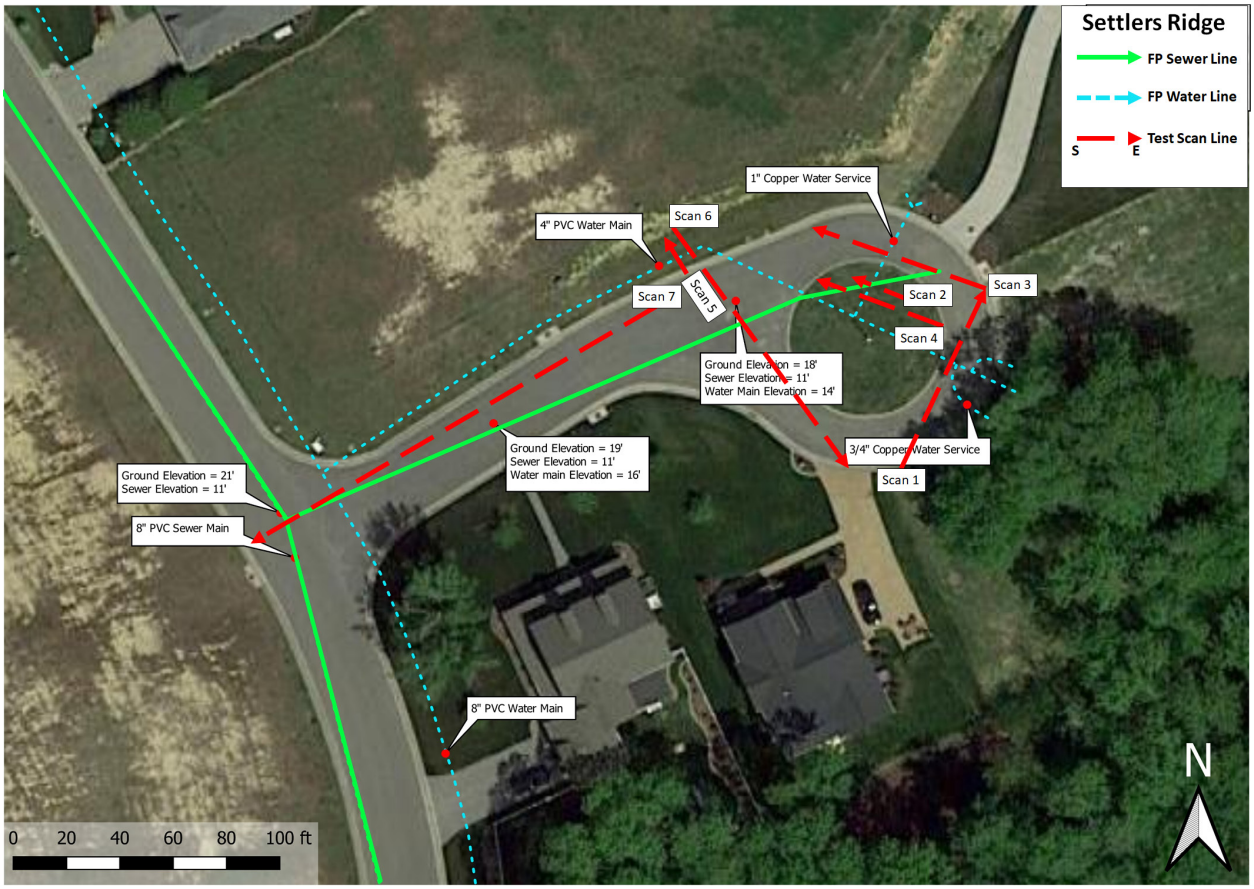


Original Photo: © 2021 Google® (see Acknowledgments section). Image modified by FHWA to identify utility types and locations.

**Figure 27. Photo. Aerial view of the Settlers Ridge field test site with utility locations, elevations, and types indicated with solid (sewer) or dashed (water) lines.**

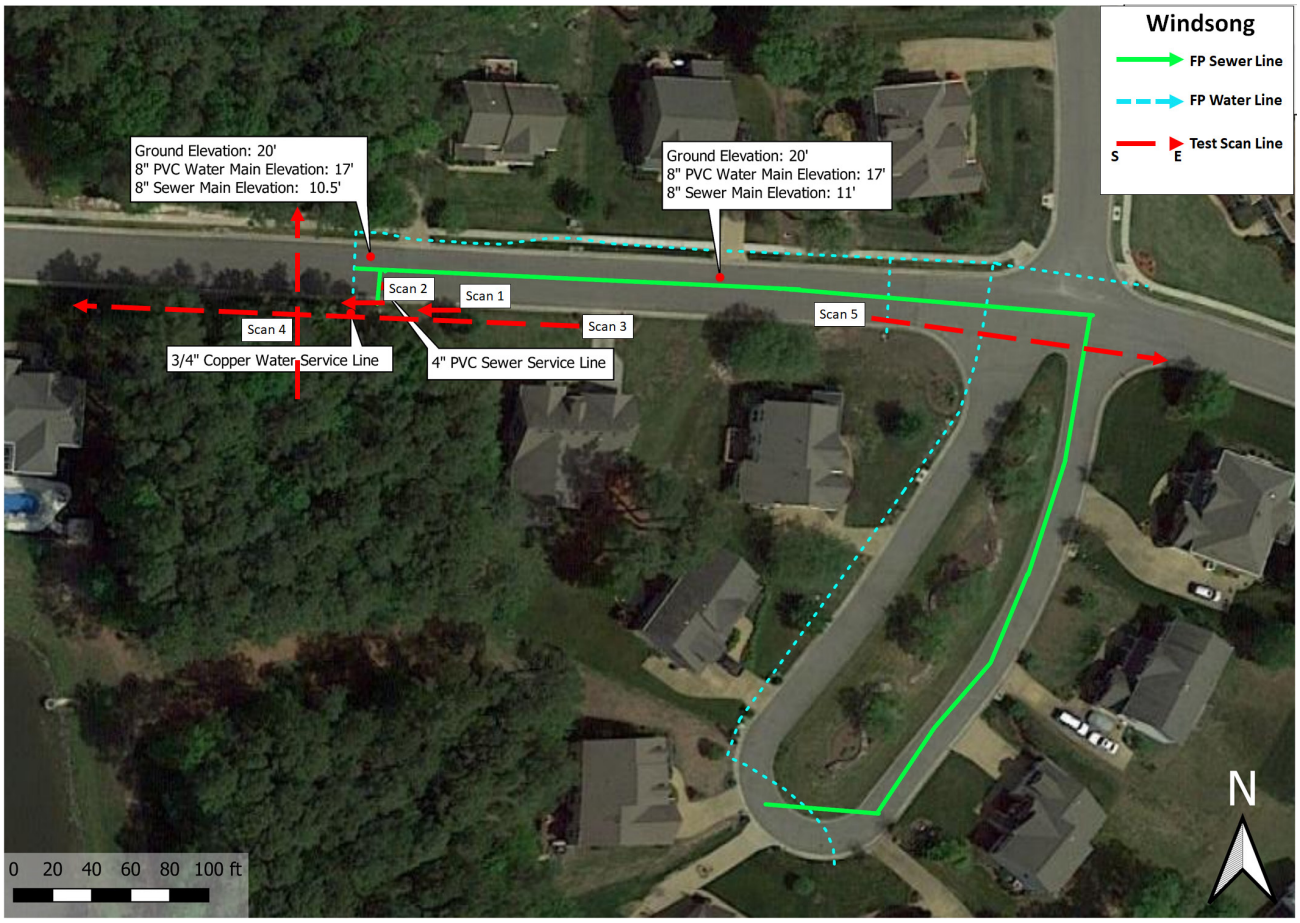


Original Photo: © 2021 Google® (see Acknowledgments section). Image modified by FHWA to identify utility types and locations.

**Figure 28. Photo. Aerial view of the Windsong Way field test site with utility locations, elevations, and types indicated with solid (sewer) or dashed (water) lines.**

## DATA ACQUISITION METHODS AND RESULTS

The field testing focused on four NDE technologies, including two EM techniques (stepped-frequency GPR and FDEM) and two seismic/acoustic techniques (MASW and APL). The following subsections provide sensor information, field plans for data acquisition, and results for GPR, MASW, APL, and FDEM ordered by their capabilities (from best to worst) to detect the buried utilities at the three sites.

### GPR Field Plan and Results

The laboratory testing used a pushcart-based, stepped-frequency GPR system that had just entered the commercial market. While this new system successfully captured features of the buried utility pipes, the raw data were difficult to access and analyze. For field tests, the project team and client elected to test another stepped-frequency GPR system and a dual-frequency (DF) GPR system with similar detection principles to the laboratory-tested system. Both field-tested systems produced data in an accessible format that made analysis straightforward.

First, the project team tested a GPR system with a DF digital antenna. The DF antenna operates simultaneously at two frequencies (300 and 800 MHz) to resolve buried utility locations. This antenna design exploits the deeper signal-penetration depth of the 300-MHz antenna and the more precise shallow feature localization of the 800-MHz antenna. In traditional applications, separate scans with each antenna would be needed to capture both datasets. The DF antenna system records two distinct signals in one scan, and the analysis software merges the scans into a final image that captures the full depth and precision from the separate frequencies.

A single technician operates the DF antenna using a four-wheeled pushcart and collects data using software on a tablet connected to the antenna. Figure 29 shows an operator deploying a DF antenna in the field. Compared to a vehicle-based or discrete point testing NDE acquisition system, the DF antenna system is mobile enough to be deployed in a variety of field conditions. This mobility was critical for the field test locations, which included roads, sidewalks, grass, and uneven ground.

In a real-world setting, the location of a buried utility pipe is not known, and GPR scans must be performed in both transverse and longitudinal directions to locate buried objects. However, to save acquisition time during the field-testing program, the team took GPR scans only in directions perpendicular to the known utility pipe orientations at the three field sites.

Source: FHWA.

**Figure 29. Photo. GPR system with DF antenna.**

The project team also deployed a stepped-frequency GPR system, which features a ground-coupled antenna and multichannel data acquisition. The stepped-frequency system is vehicle-based and typically deployed for roadway and bridge inspections. The system's

ultra-wideband frequency spectrum (200 MHz–3 GHz) makes it well-suited for buried utility location. The stepped-frequency system permits high-speed data collection and can perform up to 28 data scans in parallel during a single pass over a location. However, the stepped-frequency system cannot be used on uneven or irregular terrain and must be deployed on established roadways. This limitation hampered the utility of the stepped-frequency system during the field tests.

The stepped-frequency system also features a Global Positioning System (GPS)-based encoder that tracks the location of the antenna as it scans a test location. For this field deployment, the team used a survey system (total station) to lock down the position of the antenna. The team also leveraged the total station's GPS tracking functionality to capture the antenna coordinates along its travel path. The stepped-frequency system scans at the three testing sites covered only the roadway paths available at each site and used antenna orientations aligned with the direction of travel on the roads. Figure 30 shows the stepped-frequency GPR system on its travel vehicle along with the total station.

Source: FHWA.

**Figure 30. Photos. Photo on left shows a stepped-frequency GPR system mounted on a travel vehicle, and photo on right shows a total station surveying system used to track the GPR antenna positions.**

Analysts examined the scans from the two GPR systems to look for the distinctive time domain hyperbolic peaks produced by subsurface targets in response to radar pulses (figure 31). Each scan's observed features, GPS-encoded positions, and other field measurements were compared

to the documented locations of buried utilities to determine whether the GPR systems successfully detected the targets. Figure 31 shows an example of the interpreted results from a DF antenna GPR system scan, with yellow boxes outlining the detected utilities. The 800-MHz channel found a shallow target with high resolution, and the 300-MHz channel scan revealed two lower-resolution targets near 3 and 7 ft below the surface. The system's DF antennas collect two data channels that are displayed on separate depth-of-penetration axes. The boxes indicate features classified as buried utility pipes according to VDOT documentation.

Because the field testing involved two GPR systems with different positioning systems, the data from each test were analyzed and aggregated separately. Table 4 summarizes the DF antenna GPR system results for each scan line.

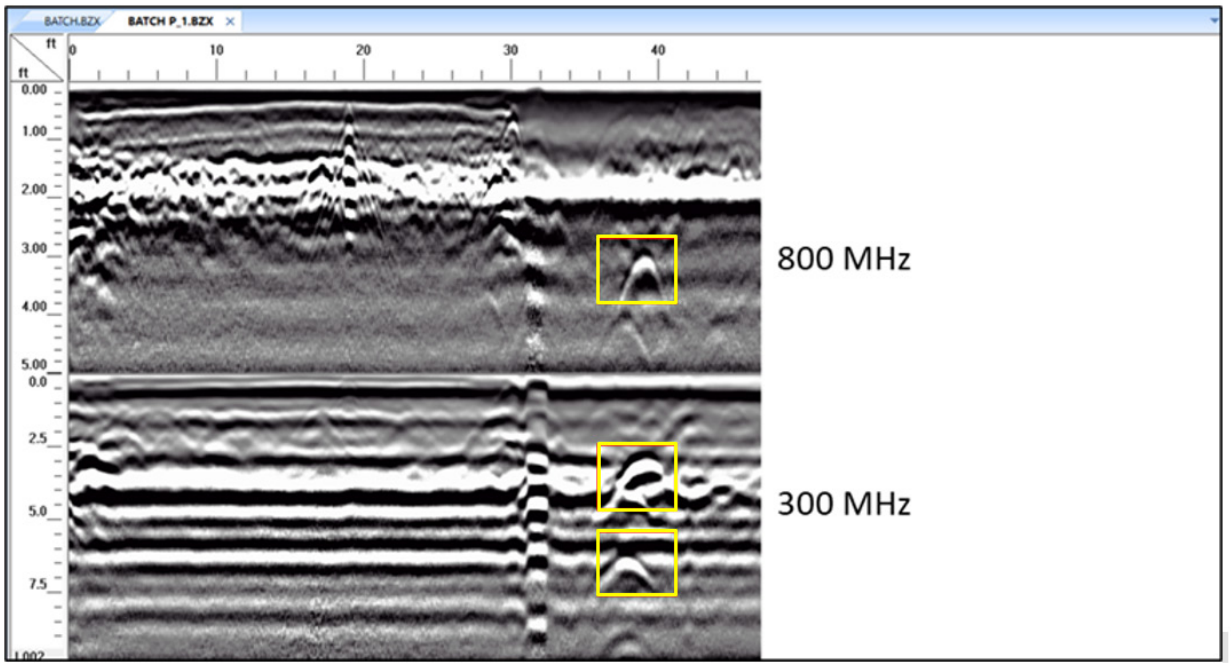


Source: FHWA.

**Figure 31. Image. Example of the DF antenna GPR scan collected during field testing at Spring Hill (scan line identification 2 in table 4).**

**Table 4. Scan line metadata and respective utility targets for the DF antenna GPR tests, including the system's success or failure to detect targets.**

| Scan Line ID | Location | Date | Primary Target | Primary Depth (ft) | Primary Target Detected? | Secondary Target | Secondary Depth (ft) | Secondary Target Detected? |
|---|---|---|---|---|---|---|---|---|
| 2 | Spring Hill | 8/24/2021 | PVC water | 3 | Yes | PVC sewer | 7 | Yes |
| 3 | Spring Hill | 8/24/2021 | PVC water | 3 | Yes | PVC sewer | 7 | No |
| 4 | Spring Hill | 8/24/2021 | PVC water | 3 | Yes | PVC sewer | 7 | Yes |
| 5 | Spring Hill | 8/24/2021 | PVC water | 3 | No | PVC sewer | 7 | No |
| 6 | Spring Hill | 8/24/2021 | PVC water | 3 | No | NA | NA | NA |
| 7 | Spring Hill | 8/24/2021 | PVC water | 3 | Yes | PVC sewer | 9 | No |
| 8 | Spring Hill | 8/24/2021 | PVC water | 3 | No | PVC sewer | 9 | Yes |
| 1 | Settlers Ridge | 8/25/2021 | Copper water | 4 | No | NA | NA | NA |
| 3 | Settlers Ridge | 8/25/2021 | Copper water | 4 | Yes | PVC sewer | 7 | No |
| 4 | Settlers Ridge | 8/25/2021 | PVC water | 4 | No | NA | NA | NA |
| 6 | Settlers Ridge | 8/25/2021 | PVC water | 4 | Yes | PVC sewer | 7 | Yes |
| 7 | Settlers Ridge | 8/25/2021 | PVC water | 3 | Yes | PVC sewer | 8 | No |
| 3 | Windsong Way | 8/26/2021 | Copper water | 3 | Yes | PVC sewer | 9.5 | No |
| 4 | Windsong Way | 8/26/2021 | PVC water | 3 | Yes | PVC sewer | 9.5 | No |
| 5 | Windsong Way | 8/26/2021 | PVC water | 3 | Yes | PVC sewer | 9 | No |

NA = Not applicable.

Several general observations can be made about the performance of the DF antenna GPR system at the three field sites. First, the system performed GPR scans in nonideal environments with variable and uneven surface conditions without a reduction in data quality or system performance. Second, the DF antenna GPR is easy to operate—a single technician can push both the antenna cart along a scan line and review data in realtime. Third, the DF antenna feature produces two channels of output at different frequencies, which provides better resolution of subsurface features. For instance, the DF antenna GPR system detected PVC water lines at relatively shallow depths, despite the nonconductive material type. However, it did not detect PVC water lines at relatively deep depths. This result is likely due to both the increased depth of pipe and the nonconductive pipe material type.

In general, the stepped-frequency GPR system did not perform as well as the DF antenna GPR system. While the stepped-frequency GPR is deployable in high-traffic settings and at typical roadway speeds, it requires considerable setup and tuning to ensure high-quality data collection.

The system benefits from GPS data encoding, which is an advantage over the DF antenna GPR, because it minimizes the need for handwritten field notes on scan start/stop positioning. The stepped-frequency GPR also detected PVC water lines at relatively shallow depths despite the nonconductive material type, but it did not detect the deeper PVC water lines due to nonconductive pipe material and the increased depth of the utility lines. Figure 32 presents an example of the stepped-frequency GPR data captured and processed in the provided data analysis software. The stepped-frequency system collects 21 parallel channels, which are displayed on both a depth plot (top photo of figure 32) and plan view scan slice (bottom photo of figure 32). The rectangular box indicates features classified as buried utility pipes according to VDOT documentation.

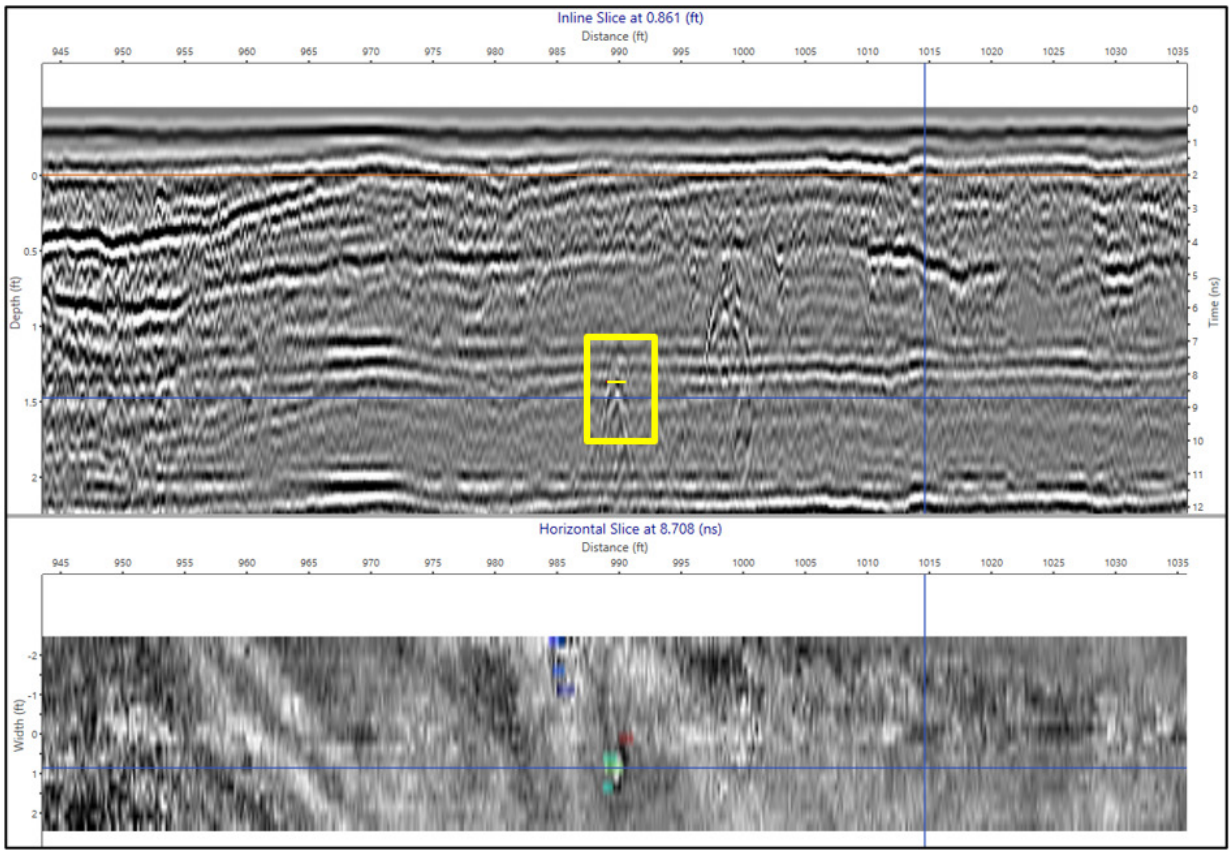


Source: FHWA.

**Figure 32. Image. Images show an example of a stepped-frequency GPR scan collected during field testing at Windsong Way.**

In contrast to the DF antenna GPR system, the stepped-frequency GPR system did not successfully map the full extent of the utilities, and many utilities were identified by only a single feature along their length. These low-quality results may have been caused by poor system orientation during scans or utility lines running outside the roadways.

### MASW Field Plan and Results

The field team used an MASW system consisting of a land streamer (i.e., inline array) with 24 vertical-component geophones and a 24-channel seismic recorder. The individual geophones in the array were coupled to the ground using spikes ("spiked" lines) or weights to allow for easier data collection ("streamer" lines), with 1-ft geophone spacing for spiked lines and 3.3-ft for streamer lines (figure 33). The MASW rental system also included a laptop computer to control the seismograph and data collection.

Source: FHWA.

**Figure 33. Photo. MASW data collection using a streamer geophone array at Settlers Ridge setup 9, deployed on asphalt.**

MASW data collection uses a strategy known as "shoot-through roll-along" acquisition that produces multiple seismic records (collections of time histories) with the same source-to-receiver offsets and geophone array lengths. Each acquisition layout is designed for a specific investigation depth to maximize the accuracy of the final subsurface images. For the field tests, the MASW team tried three MASW data-acquisition strategies. One approach involved having six source locations on the ends of the array at various offsets (noted as "standard" approach in table 5). The second method was a shoot-through approach that involved moving the source through the geophone array, also known as roll-along. The third method was a partial shoot-through approach that involved moving the source through the center of the array. Figure 34 depicts the most successful acquisition setup to detect buried utilities (setup 2).

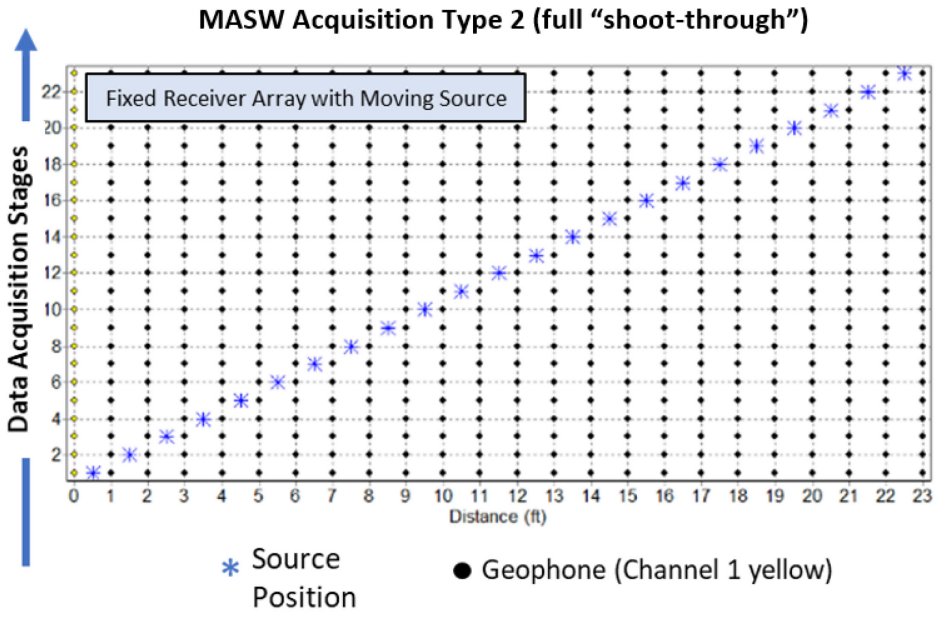


Source: FHWA.

**Figure 34. Graph. MASW data-acquisition strategy used during field testing denotes a "shoot-through" approach where the geophone array remained in place and the source positions varied.**

To induce ground motion, the field crew employed 1.5-lb and 4-lb double-ended metal hammers to strike metal plates on the ground. These lightweight sources were sufficient for the shallow targets of interest (under approximately 13 ft). The data records were stacked over three hammer swings per source location to increase the data signal-to-noise ratio. Field personnel designed the layout at each setup to detect a primary target near the middle of the geophone array and a secondary target (if one existed) closer to an end of the array. The team conducted five or more layouts at each of the three testing locations (Spring Hill, Settlers Ridge, and Windsong Way) using the streamer and/or spiked geophone line on targets of various diameter, material, and estimated depth (table 5).

The postacquisition analysis of MASW data follows a multistep processing procedure to generate a 2D image of the subsurface shear-wave velocities ($V_S$). In the first step, surface-wave dispersion analysis is performed on the waveforms recorded at each geophone position to capture the behavior of the surface waves as a function of frequency. Then, dispersion curves are selected and inverted to produce one-dimensional (1D) $V_S$ profiles, and the 1D $V_S$ profiles are interpolated to create a final 2D $V_S$ image (Park et al. 2007). Buried subsurface objects show up as low-$V_S$ anomalies in the final MASW results.

As a general rule of thumb, the MASW technology can resolve underground feature diameters greater than approximately 30 percent of their emplacement depth. For example, MASW can resolve a 1-ft diameter pipe if its depth is less than 3.3 ft. It is possible to achieve finer resolution

for shallow targets, but higher resolution is largely dependent on geophone spacing along the MASW array.[1]

To determine the range of conditions over which MASW detected buried utilities, the field team acquired MASW data with different hammer-source weights and geophone spacing over pipes with various diameters and emplacement depths. The field tests conclusively showed that the shoot-through approach data-acquisition strategy was the only successful layout used to detect buried utilities. Unfortunately, most of the MASW data were collected using setup 1 ("standard") acquisition layout, and most of the utilities were too small or deep to be detected successfully.

[1]Dr. Choon Park, personal communication, 2021.

## Table 5. MASW experimental setups and utility detection results.

| Setup No. | Location | Line Type | Setup | Primary Target | Primary Diameter (inches) | Primary Depth (ft) | Primary Target Detected? | Secondary Target | Secondary Diameter (inches) | Secondary Depth (ft) | Secondary Target Detected? |
|---|---|---|---|---|---|---|---|---|---|---|---|
| 1 | Spring Hill | Streamer | Standard | PVC water | 8 | 3 | N | PVC sewer | 8 | 7 | N |
| 2 | Spring Hill | Streamer | Standard | PVC sewer | 8 | 7 | N | PVC water | 8 | 3 | N |
| 3 | Spring Hill | Streamer | Standard | PVC water | 8 | 3 | N | PVC sewer | 8 | 9 | N |
| 4 | Spring Hill | Streamer | Standard | PVC sewer | 8 | 3 | N | — | — | — | — |
| 5 | Spring Hill | Streamer | Standard | PVC water | 8 | 3 | N | — | — | — | — |
| 6 | Settlers Ridge | Spike | Standard | PVC water | 4 | 4 | N | — | — | — | — |
| 7 | Settlers Ridge | Spike | Shoot-through approach | PVC water | 4 | 4 | Y | — | — | — | — |
| 8 | Settlers Ridge | Streamer | Standard | PVC water | 4 | 4 | N | — | — | — | — |
| 9 | Settlers Ridge | Streamer | Partial shoot-through approach | PVC sewer | 8 | 10 | N | — | — | — | — |
| 10 | Settlers Ridge | Streamer | Standard | PVC water | 8 | 4 | N | PVC sewer | 8 | 10 | N |
| 11 | Settlers Ridge | Streamer | Shoot-through approach | PVC sewer | 8 | 10 | Y | PVC water | 8 | 4 | Y |
| 12 | Settlers Ridge | Streamer | Standard | PVC sewer | 8 | 10 | N | PVC water | 8 | 1 | N |
| 13 | Windsong Way | Spike | Standard | PVC sewer | 4 | 1.5 | N | Copper water | 0.75 | 1 | N |
| 14 | Windsong Way | Spike | Standard | PVC sewer | 4 | 1.5 | N | Copper water | 0.75 | 9.5 | N |
| 15 | Windsong Way | Streamer | Standard | PVC water | 8 | 3 | N | PVC sewer | 8 | — | N |
| 16 | Windsong Way | Streamer | Standard | PVC sewer | 8 | 9.5 | N | — | — | — | — |
| 17 | Windsong Way | Streamer | Standard | PVC water | 8 | 3 | N | — | — | — | — |
| 18 | Windsong Way | Streamer | Standard | PVC sewer | 8 | 9.5 | N | — | — | — | — |

—No data.

### *MASW Example Results—Settlers Ridge Setup Number 11 (SR11)*

For SR11 in table 5, the field team used the partial shoot-through data-acquisition approach. A commercial software package was used to process MASW data by using 12 geophone traces at a time and sweeping through the waveform dispersion analysis. An analyst manually selected a 1D dispersion curve for each geophone location, and the software inverted the curves to produce a 2D shear-velocity map. MASW theory dictates that buried utilities should appear as low-velocity zones in the 2D shear-wave velocity images. The SR11 results in figure 35 show two low-velocity zones that correlate well with the expected depths of the water and sewer pipes.

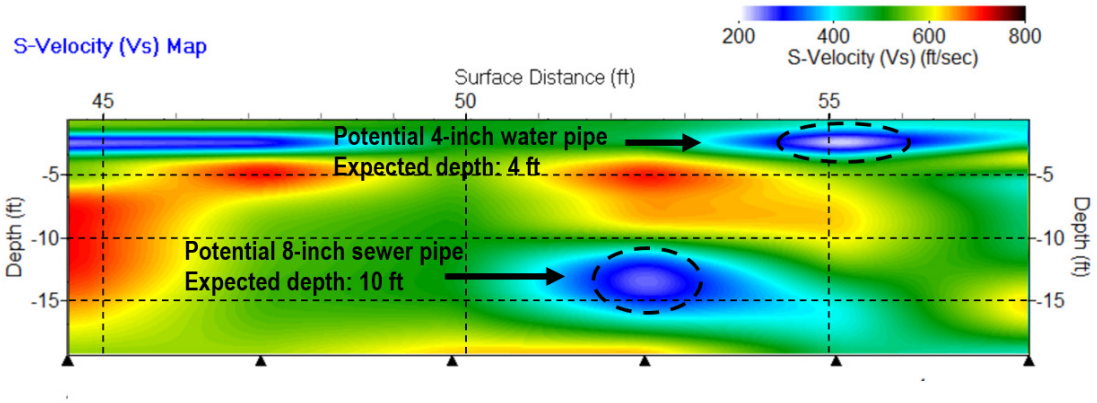


Source: FHWA.

**Figure 35. Image. SR11 2D shear-velocity profile versus depth. Two anomalous low-velocity zones appear near the expected locations of buried utility lines (Jalinoos 2022).**

At this site, an 8-inch PVC sewer line is located at a depth of 10 ft, but the 2D MASW image places it closer to 13 ft. The site maps indicate a 4-inch PVC water pipe at a depth of 4 ft. MASW located it closer to a 3-ft depth. These results indicate the usefulness of MASW to detect and approximately locate utility lines, although the pipe diameter is not well constrained using standard processing techniques.

### *MASW Example Results—Settlers Ridge Setup Number 7 (SR7)*

At the SR7 site, the field team used a full shoot-through approach with a 1-ft geophone spacing to detect a shallow target. The same MASW processing procedure used for SR11 was applied to the SR7 data. The analyst manually selected a full set of dispersion curves and performed inversion to generate the final $V_S$ profile shown in figure 36. For the SR7 setup, a low-velocity zone was identified near the location and depth expected of the 4-inch water pipe (figure 36).

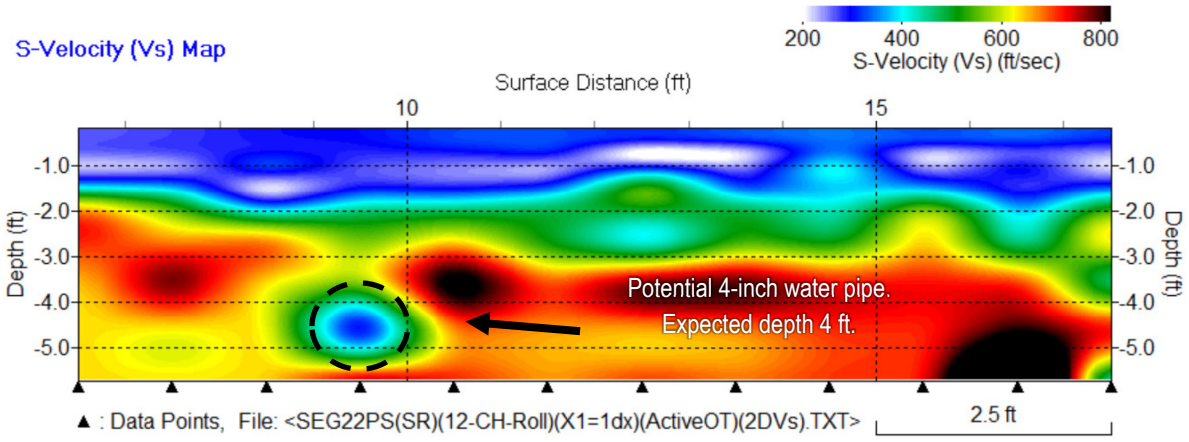


Source: FHWA.

**Figure 36. Image. SR7 2D shear wave velocity profile showing an anomalous low-velocity zone near the depth of the target pipe (4-inch PVC water line).**

### *Summary of MASW Results*

The results provide evidence that MASW technology can detect and approximately locate utility lines, particularly with the right acquisition strategies and streamer array parameters. Specifically, using the shoot-through MASW acquisition strategies led to clear detections of utilities at Settlers Ridge setups 11 and 7, including 4-inch water lines at 3.3- and 4-ft depths and an 8-inch sewer line at a depth of 10 ft. Geophone spacing and the appropriate source weights are key parameters for a successful application of MASW to detect buried utilities.

Furthermore, while the MASW method can successfully image the locations and depths of buried utilities, it is unable to resolve pipe diameters with confidence. The MASW technology is still not suitable as a standalone detection method of underground utilities, but it can be used as an auxiliary method to increase confidence in the results from other NDE technologies or as an alternative method when GPR or other methods are unsuccessful.

### APL Field Plan and Results

The field team expected the APL to perform poorly at the Virginia test sites, which consisted primarily of paved or concrete surfaces. In these settings, acoustic waves experience high attenuation due to the stiff surface media, and soil inhomogeneities beneath the surface, such as air voids, increase uncertainties in APL measurements. With these limitations in mind, the team selected APL scan lines perpendicular to known buried utilities and prioritized acquisition locations with soil rather than pavement. The crew collected APL measurements every 6 inches along the length of each scan line, with the APL tool oriented perpendicular to buried utility lines. Figure 37 shows an image of the APL instrument in use.

Source: FHWA.

**Figure 37. Photo. APL system in use during field testing.**

Analysis of the APL data involved a review of the acoustic responses gathered during testing to identify the presence of anomalies that might indicate a buried utility. Pipe detection with the APL instrument requires multiple field conditions to be met—the most important is a difference in subsurface sound speed between the pipe and the surrounding soil. While some APL scans revealed impedance mismatches in the acoustic signatures, their locations did not generally align with known subsurface target positions. Many of the field site utilities were buried beneath roadways and sidewalks, where the APL tool is known to be less effective. Even the APL scans performed over soil produced noisy signatures that made it impossible to identify features related to buried utilities confidently. Figure 38 presents a typical example of the APL data collected during the VDOT field tests.

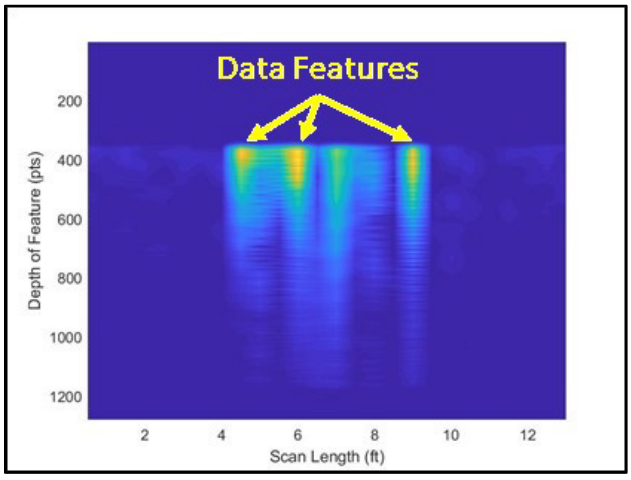


Source: FHWA.

**Figure 38. Image. Example of an APL scan collected during field testing.**

### FDEM Instrument Field Plan and Results

The project team used a frequency-domain ground conductivity meter to collect FDEM measurements. The FDEM-based instrument is sensitive to changing soil conditions, and

variations in surface conditions or subsurface geological layers can present challenges for system accuracy. In general, the instrument operates in a similar fashion to GPR: it is most sensitive to conductive buried objects and produces a signal feature that shows up as a contrast from the background. FDEM's advantage is that the system presents no logistical challenges for data collection because it is completely mobile and unaffected by terrain. Because the buried utility lines at the three VDOT field sites were mostly made of PVC, the FDEM instrument's performance was substandard.

The team collected FDEM data along the same scan lines used for the GPR data collection (i.e., scan lines perpendicular to the buried utility pipes) with the instrument oriented in the horizontal direction. A GPS unit connected to the data-collection system tracked the position of the instrument during each scan. Figure 39 presents an image of the FDEM conductivity meter in use during field tests.

Source: FHWA.

**Figure 39. Photo. FDEM system in use during field testing.**

Analysis of the FDEM data involves a review of relative conductivity measurements made along linear scan paths. The presence of significant conductivity minima in the data indicate the presence of a conductive pipe. Figure 40 presents a typical example of FDEM data collected along a Settlers Ridge scan line with known PVC subsurface targets. Variable surface conditions near the scan path's start point (approximately 0–10 ft) likely caused the initial variability of the relative conductivity measurements. The measurements varied less as the FDEM instrument encountered a more uniform section of roadway. Buried utilities should show up as significant negative peaks relative to average, but this particular scan did not reveal any subsurface features of note. The VDOT field sites generally contained nonconductive PVC utility lines, and consequently, none of the FDEM scans successfully detected any buried utility lines. These

results mirror the findings in the soil box laboratory work, where a similar FDEM system was unsuccessful in detecting PVC pipes.

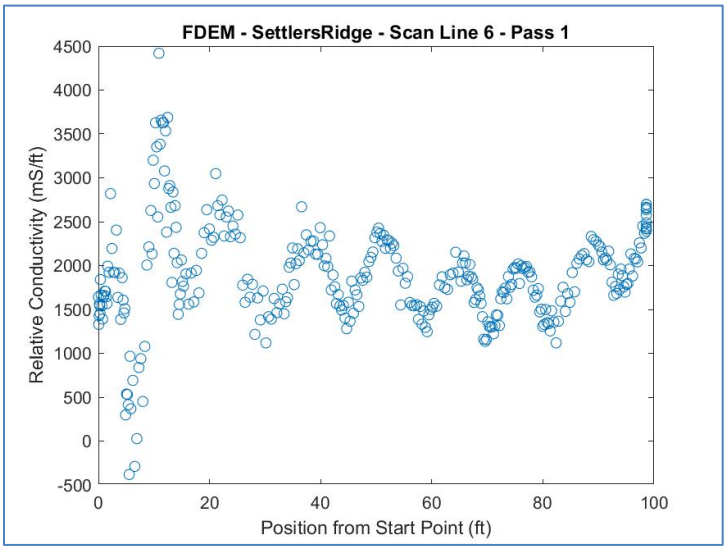


Source: FHWA.

**Figure 40. Image. Typical example of an FDEM scan collected during field testing (Settlers Ridge, scan line 6).**

## FIELD TEST CONCLUSIONS

The field tests conducted at three VDOT sites mostly confirmed the soil box laboratory results discussed previously, although the three sites presented significantly tougher conditions than expected, particularly for the EM NDE technologies (GPR and FDEM).

The GPR field results varied significantly depending on the particular system used. In general, the DF antenna system fared much better than the stepped-frequency system. This was mostly due to the stepped-frequency system's restricted use to paved roadways, but even when used on roadways, the stepped-frequency system was incapable of tracking utility lines below approximately 3.5 ft. In contrast, the DF antenna GPR found utilities at most testing sites. The DF antenna feature of the GPR system increased subsurface resolution and penetration depths, which allowed nonconductive utility pipes to be found in several scans.

The MASW method successfully detected and located buried utilities, but only when the field team implemented a survey design that increased the signal-to-noise ratios of the surface waves propagating directly over the presumed utility locations. Although not presented in this report, the MASW data also showed indications of higher-mode, surface-wave energy that could enhance the 2D subsurface $V_S$ images and provide greater certainty of utility location and depth. Additional research and fieldwork are suggested to confirm the success of MASW for locating buried utilities and the variable setup parameters required to detect pipes of different diameters at various depths.

# CHAPTER 6. NDE TECHNOLOGY RECOMMENDATIONS

This study produced several recommended NDE technologies that are capable of detecting and locating buried utilities. GPR remains the most reliable and consistent NDE method available for the buried utility application, while the use of the FDEM was not applicable as the field test sites did not offer any conductive utility pipes for detection. In addition, the study results mostly demonstrate the current state of the art in GPR technology (multifrequency GPR and stepped-frequency GPR), as GPR is already an established method for utility location.

Although data were gathered in line with the standard procedures and settings for the system, APL was inconclusive in the detection of any buried utilities in either laboratory or field-testing conditions. It may be possible for the APL data-acquisition strategies to be improved to increase their relevance for the buried utility application, or perhaps these data types could supplement the results from GPR or MASW. Various field conditions could have influenced the APL readings as well, such as inhomogeneous soil conditions that interfered with the built-in processing methods.

Seismic methods such as MASW proved to be a new emerging technology for NDE based on success at locating the buried utilities at the Windsong Way field site in southern Virginia. MASW should not yet be considered a standalone NDE technology for buried utility detection and location, but it is the most promising non-GPR technology investigated so far. Further investigation of best-practice acquisition strategies and improved data processing could place MASW well ahead of other NDE technologies, particularly for nonconductive pipe materials emplaced at depths below approximately 4 ft.

By conducting fundamental, comprehensive research of existing and emerging NDE technologies, this project successfully tested and identified various NDE technologies to detect and locate various buried utilities. Table 6 lists the various technologies, their setup parameters, ideal testing conditions, and the project team's recommendations.

**Table 6. Recommendations of NDE technologies.**

| Method | Technology | Suggested Setup and Usage Parameters | Ideal Conditions | Recommendations |
|---|---|---|---|---|
| **GPR** | Multifrequency impulse GPR | Use wide spectral band wherever possible; prioritize low frequencies in the 100–400 MHz range. | Homogeneous soil conditions with little to no clay. | Multifrequency and stepped-frequency GPR recommended for detection of buried utilities, particularly for metallic pipes. |
| | Stepped-frequency GPR | Use operator-driven GPR for rugged and nonideal field conditions. | Dry environments. | |
| | | Use vehicle-mounted GPR under ideal conditions for high-speed data collection. | Relatively flat, firm, and even surface conditions for scanning. | |
| **EM technologies** | Pipe and cable locators | Cycle through frequency-detection modes on the locator to identify most effective for a utility type. | Homogeneous soil conditions with little to no clay. | Recommended for detecting active cables or where connection can be made to the buried utility to support the locator. |
| | | | Dry environments. | Passive location modes not recommended for detecting unpowered utilities. |
| | FDEM method | Cycle through frequency-detection modes on the locator to identify most effective for a utility type. | Homogeneous soil conditions with little to no clay. | Recommended for detection of shallow metallic pipes; lack of a real-time display reduces its effectiveness for utility location. |
| | | | Dry environments. | |
| | | | Relatively flat, firm, and even surface conditions for scanning. | |

| Method | Technology | Suggested Setup and Usage Parameters | Ideal Conditions | Recommendations |
|---|---|---|---|---|
| **Acoustic technologies** | APL | Select 6-inch instrument spacing to ensure an effective density of data points. | Homogeneous soil conditions with little to no clay. | Inconclusive for utility detection. |
| | | Select deep-mode data collection to ensure instrument captures effective depth. | Dry environments. | |
| | | | Relatively flat, soft, and even surface conditions for scanning. | |
| **Seismic technologies** | MASW | Minimum of 24 geophones and a shoot-through approach recommended. | Pipe depths from 3 to 12 ft. | MASW recommended for further testing with shoot-through acquisition geometry. |
| | | Source weight between 1.5 and 4 lb for pipes <15 ft. | Sensor locations on soil, grass, or asphalt. | |
| | | | Good impedance contrast between utility and soil. | |
| | HVSR | Requires at least four broadband sensors at a minimum spacing equal to pipe diameter. | General location of utilities must be known due to the time required to apply the technique (approximately 30 min/site). | Inconclusive for utility detection. |

## ACKNOWLEDGMENTS

Figure 4 is republished with permission of Elsevier Science & Technology Journals, from "Testing the Horizontal to Vertical Spectral Ratio Technique as a Tool for Utility Detection" by A. Khalil, G. Anukwu, and M. Nordin in the *Journal of Applied Geophysics*, volume 173, 2020. Permission conveyed via Copyright Clearance Center, Inc.

The maps in figure 26, figure 27, and figure 28 in this document were modified. The original maps are the copyright property of Google® Earth™ and can be accessed from https://www.google.com/earth/ (Google® 2021). The map overlays showing the placement of utility locations, elevations, and type indicated with green (sewer) or cyan (water) dashed lines were developed as part of this research project.

## REFERENCES


Al-Shayea, N. A., R. D. Woods, and P. Gilmore. 1994. "SASW and GPR to Detect Buried Objects." *Proceedings of the Symposium on the Application of Geophysics to Engineering and Environmental Problems.* Wheat Ridge, CO: Environmental and Engineering Geophysical Society.

Anspach, J. 1995. "Subsurface Utility Engineering: Upgrading the Quality of Utility Information." *Proceedings of the International Conference on Advances in Underground Pipeline Engineering*. New York, NY: American Society of Civil Engineers (ASCE).

ASCE. 2002. *Standard Guidelines for the Collection and Depiction of Existing Subsurface Utility Data*. New York, NY: American Society of Civil Engineers, Codes and Standards Activity Committee.

Badsar, S., M. Schevenels, W. Haegeman, and G. Degrande. 2010. "Determination of the Material Damping Ratio in the Soil from SASW Tests Using the Half-Power Bandwidth Method." *Geophysical Journal International* 182: 1493–1508.

Chemekoff, J., and D. Toussaint. 1994. "Pipe Location Technology Has Rich History." *Water Engineering and Management* 141, no. 4: 28–31.

Daniels, D. (Ed.). 2004. *Ground Penetrating Radar* (second ed., Vol. 1). London: The Institution of Electrical Engineers.

Datta, S., and S. Sarkar. 2016. "A Review on Different Pipeline Fault Detection Methods." *Journal of Loss Prevention in the Process Industries* 41: 97–106.

Dolphin, L. 1997. *Ground Penetrating Radar (GPR) Usage and Limitations*. Retrieved from Lambert Dolphin Library. http://www.ldolphin.org/GPRLimits.html, last accessed August 25, 2022.

European Commission—Research General Directorate. 2004. "Guidelines for the Implementation of the H/V Spectral Ratio Technique on Ambient Vibrations Measurements, Processing, and Interpretation." *No. EVG1-CT-2000-00026 SESAME*. 62. Brussels, Belgium: European Commission.

Fernández, J., L. Hermanns, A. Fraile, E. Alarcón, and I. Del Rey. 2011. "Spectral Analysis Surface Waves Method in Ground Characterization." *Procedia Engineering* 10: 3202–3207.

García-Jerez, A., J. Piña-Flores, F. J. Sánchez-Sesma, F. Luzón, and M. Perton. 2016. "A Computer Code for Forward Calculation and Inversion of the H/V Spectral Ratio Under the Diffuse Field Assumption." *Computers & Geosciences* 97: 67–68.

GEOVision. 2016. *Spectral Analysis of Surface Waves Method*. Retrieved July 2020, from GEOVision Geophysical Services: www.geovision.com.

Google®. 2021. *Google® Earth™*. Retrieved from https://www. google.com/earth.

Grandjean, G., J. C. Gourry, and A. Bitri. 2000. "Evaluation of GPR Techniques for Civil-Engineering Applications: Study on a Test Site." *Journal of Applied Geophysics* 45*,* no. 3: 141–156.

Grivas, D. A. 2006. *Applications of Ground Penetrating Radar for Highway Pavements.* Institute for Infrastructure Asset Management. Latham, NY: New York State Department of Transportation.

Hammon III, W. S., G. A. McMechan, and X. Zeng. 2000. "Forensic GPR: Finite-Difference Simulations of Responses from Buried Human Remains." *Journal of Applied Geophysics* 45, no. 3: 171–186.

Hamran, S. E., T. Guneriussen, J. O. Hagen, and R. Odegard. 1997. "Ground Penetration Radar and ERS SAR Data for Glacier Monitoring." *International Geoscience and Remote Sensing Symposium Proceedings* 2: 634–636. IGARSS'97. Piscataway, NJ: Institute of Electrical and Electronics Engineers (IEEE).

Hamran, S., and K. Langley. 2004. "A 5.3 GHz Step-Frequency GPR for Glacier Surface Characterisation." *Proceedings of the Tenth International Conference on Ground Penetrating Radar*: 761–764. IEEE. Piscataway, NJ: IEEE.

Hawari, A., M. Khader, W. Hirzallah, T. Zayed, and O. Moselhi. 2017. "Integrated Sensing Technologies for Detection and Location of Leaks in Water Distribution Networks." *Water Science and Technology: Water Supply* 17, no. 6: 1589–1601.

Hubbard, S., J. Chen, K. Williams, Y. Rubin, and J. Peterson, J. 2005. "Environmental and Agricultural Applications of GPR." *Proceedings of the 3rd International Workshop on Advanced Ground Penetrating Radar*: 45–49. IEEE. Piscataway, NJ: IEEE.

Hutchinson, P. J., and M. H. Beird. 2016. "3D Mapping with MASW." *The Leading Edge* 35*,* no. 4: 350–352.

Jalinoos, F. 2022. *TechBrief: Availability, Feasibility, and Reliability of Available Nondestructive Evaluation Technologies for Detecting and Locating Buried Utilities*. FHWA-HRT-22-111. Washington, DC: Federal Highway Administration.

Jaw, S. W., and M. Hashim. 2013. "Locational Accuracy of Underground Utility Mapping Using Ground Penetrating Radar." *Tunnelling and Underground Space Technology* 35: 20–29.

Jeng, Y., and C.-S. Chen. 2012. "Subsurface GPR Imaging of a Potential Collapse Area in Urban Environments." *Engineering Geology* 147: 57–67.

Jeong, H. S., and D. M. Abraham. 2004. "A Decision Tool for the Selection of Imaging Technologies to Detect Underground Infrastructure." *Tunnelling and Underground Space Technology* 19, no. 2: 175–191.

Kavi, J. 2018. *Detection of Buried Non-Metallic (Plastic and FRP Composite) Pipes Using GPR and IRT.* Graduate Theses, Dissertations, and Problem Reports. 3724. West Virginia University.

Khalil, A. E., G. C. Anukwu, and M. N. Nordin. 2020. "Testing the Horizontal to Vertical Spectral Ratio Technique as a Tool for Utility Detection." *Journal of Applied Geophysics* 173: 10398.

Lai, W. W.-L., X. Dérobert, and P. Annan. 2018. A Review of Ground Penetrating Radar Application in Civil Engineering: A 30-Year Journey from Locating and Testing to Imaging and Diagnosis. *NDT&E International* 96: 58–78.

Langman, A., and M. R. Inggs. 1998. "A 1-2 GHz SFCW Radar for Landmine Detection." *Proceedings of the 1998 South African Conference on Communications and Signal Processing-COMSIG'98*: 453–454. IEEE. Piscataway, NJ: IEEE.

Lin, C. P., C. H. Lin, and C. J. Chien. 2017. "Dispersion Analysis of Surface Wave Testing–SASW vs. MASW." *Journal of Applied Geophysics* 143: 223–230.

Liu, Y., D. Habibi, D. Chai, X. Wang, H. Chen, Y. Gao, and S. Li. 2020. "A Comprehensive Review of Acoustic Methods for Locating Underground Pipelines." *Applied Sciences* 10, no. 3: 1031.

Manacorda, G., H. Scott, P. D. Loach, J. J. Kazik, D. Pinchbeck, M. Remeil, J. Capdevielle, and P. Fournier. 2004. "The European GIGA project." *Proceedings of the Tenth International Conference on Ground Penetrating Radar (GPR)* 1: 355–358. IEEE. Piscataway, NJ: IEEE.

Mendecki, M. J., B. Bieta, and M. Mycka. 2014. "Determination of the Resonance Frequency-Thickness Relation Based on the Ambient Seismic Noise Records from Upper Silesia Coal Basin." *Contemporary Trends in Geoscience* 3, no. 1: 41–51.

Metje, N., P. R. Atkins, M. J. Brennan, D. N. Chapman, H. M. Lim, J. Machell, and A. M. Thomas. 2007. "Mapping the Underworld–State-of-the-Art Review." *Tunnelling and Underground Space Technology* 22: no. 5–6, 568–586.

Metwaly, M. 2015. "Application of GPR Technique for Subsurface Utility Mapping: A Case Study from Urban Area of Holy Mecca, Saudi Arabia." *Measurement* 60: 139–145.

Miller, R. D., C. B. Park, J. M. Ivanov, J. Xia, D. R. Laflen, C. Gratton, and R. Overton. 2000. *MASW to Investigate Anomalous Near-Surface Materials at the Indian Refinery in Lawrenceville, Illinois.* Open-File Report No. 2000-4. Lawrence, KS: Kansas Geological Survey. https://www.kgs.ku.edu/, last accessed September 9, 2022.

Moorman, B. J., and F. A. Michel. 2000. "Glacial Hydrological System Characterization Using Ground-Penetrating Radar." *Hydrological Processes* 14, no. 15: 2645–2667.

Nakamura, Y. 1989. “A Method for Dynamic Characteristics Estimation of Subsurface Using Microtremor on the Ground Surface.” *Railway Technical Research Institute, Quarterly Reports* 3, no. 1.

Neal, A. 2004. “Ground-Penetrating Radar and Its Use in Sedimentology: Principles, Problems and Progress.” *Earth-Science Reviews* 66, no. 3–4: 261–330.

Papandreou, B., E. Rustighi, and M. J. Brennan. 2008. *A Study into the Feasibility of Using Acoustic Techniques to Locate Buried Objects.* ISVR Technical Memorandum No. 979. University of Southampton Institute of Sound and Vibration Research.

Park, C. B., R. D. Miller, and J. Xia. 1996. “Multi-Channel Analysis of Surface Waves Using Vibroseis (MASWV).” *SEG Technical Program Expanded Abstracts 1996.* 68–71. Society of Exploration Geophysicists.

Park, C. B., R. D. Miller, and J. Xia. 1999. “Multichannel Analysis of Surface Waves.” *Geophysics* 64, no. 3: 800–808.

Park, C. B., R. D. Miller, J. Xia, and J. Ivanov. 2007. “Multichannel Analysis of Surface Waves (MASW)—Active and Passive Methods.” *The Leading Edge* 26, no. 1: 60–64.

Park, C. B., R. D. Miller, M. Brohammer, J. Xia, and J. Ivanov. 2000. *Using SurfSeis© 2000 for Multichannel Analysis of Surface Waves (MASW): User’s Manual.* Lawrence, KS: Kansas Geological Survey, October. https://www.kgs.ku.edu/software/surfseis/SurfSeisMan.pdf, last accessed December 21, 2022.

Park, Y. J., K. H. Kim, S. B. Cho, D. W. Yoo, D. G. Youn, and Y. K. Jeong. 2003. “Development of a UWB GPR System for Detecting Small Objects Buried Under Ground.” *Proceedings of IEEE Conference on Ultra Wideband Systems and Technologies*: 384–388. IEEE. Piscataway, NJ: IEEE.

Park, Y. J., K. H. Kim, S. B. Cho, D. W. Yoo, D. G. Youn, and Y. K. Jeong. 2004. October. “Buried Small Objects Detected by UWB GPR.” *IEEE Aerospace and Electronic Systems Magazine* 19, no. 10: 3–6.

Plewes, L. A., and B. Hubbard. 2001. “A Review of the Use of Radio-Echo Sounding in Glaciology.” *Progress in Physical Geography* 25, no. 2: 203–236.

Sauret, E. S. G., J. Beaujean, F. Nguyen, S. Wildemeersch, and S. Brouyere. 2015. “Characterization of Superficial Deposits Using Electrical Resistivity Tomography (ERT) and Horizontal-to-Vertical Spectral Ratio (HVSR) Geophysical Methods: A Case Study.” *Journal of Applied Geophysics* 121: 140–148.

Scheers, B., M. Piette, and A. Vander Vorst. 1998. “The Detection of AP Mines Using UWB GPR.” *Second International Conference on Detection of Abandoned Land Mines.* 50–54. London, UK: The Institution of Engineering and Technology (IET).

Sciotti, M., F. Colone, D. Pastina, and T. Bucciarelli. 2003. “GPR for Archaeological Investigations: Real Performance Assessment for Different Surface and Subsurface Conditions.” *IGARSS IEEE. 2003 International Geoscience and Remote Sensing Symposium Proceedings* 4. IEEE. Piscataway, NJ: IEEE.

Sterling, R. L., J. Anspach, E. Allouche, J. Simicevic, C. D. Rogers, K. E. Weston, and K. Hayes. 2009. *Encouraging Innovation in Locating and Characterizing Underground Utilities.* Report S2-R01-RW. Washington, DC: The National Academies Press. SHRP 2 Transportation Research Board.

Talwani, M., and W. Kessinger. 2003. Exploration Geophysics. In *Encyclopedia of Physical Science and Technology*. Third ed. 709–726. San Diego: CA: Academic Press.

Telford, W. M., L. P. Geldart, and R. E. Sheriff. 1990. *Applied Geophysics.* Second ed. Cambridge, UK: Cambridge University Press.

Thompson, E. M., L. G. Baise, Y. Tanaka, and R. E. Kayen. 2012. “A Taxonomy of Site Response Complexity.” *Soil Dynamics and Earthquake Engineering* 41, no. 32–43.

Vickridge, I. G., and D. Leontidis. 1997. Sewer Surveys. In *Sewers—Rehabilitation and Construction Repair* Vol. 1 Repair and Renovation. 84–102. London: Arnold.

Wightman, W. E., F. Jalinoos, P. Sirles, and K. Hanna. 2003. *Application of Geophysical Methods to Highway Related Problems.* FHWA-IF-04-021. Lakewood, CO: Federal Highway Administration Central Federal Lands Highway Division.

Xia, J., R. D. Miller, and C. B. Park. 1999. “Estimation of Near-Surface Shear-Wave Velocity by Inversion of Rayleigh Waves.” *GEOPHYSICS* 64, no. 3: 691–700.

Xia, J., R. D. Miller, C. B. Park, J. Hunter, D. Laflen, R. Good, and C. Gratton. 1998. *Comparison of Shear Wave Velocities from MASW Technique and Borehole Measurements in Unconsolidated Sediments of the Fraser River Delta.* Open-file Report 98-58. Lawrence, KS: Kansas Geological Survey.

Xiaojian, Y., Y. Haizhong, and W. Huiliang. 1997. “The Applications of GPR to Civil Engineering in China.” *IGARSS'97. 1997 IEEE International Geoscience and Remote Sensing Symposium Proceedings. Remote Sensing—A Scientific Vision for Sustainable Development* 1: 232–234. IEEE. Piscataway, NJ: IEEE.

Yarovoy, A., A. Schukin, I. Kaploun, and L. Ligthart. 2003. “Multi-Waveform Full-Polarimetric Video Impulse Radar for Landmine Detection.” *2003 33rd European Microwave Conference* 1003–1006. IEEE. Piscataway, NJ: IEEE.

Young, G. N., and C. M. Kennedy. 2015. *Utility Locating Technology Development Using Multisensor Platforms.* No. SHRP 2 Report S2-R01B-RW-1. Washington, DC: The Transportation Research Board of the National Academies of Sciences, Engineering, and Medicine.

Recycled
Recyclable

Recommended citation: Federal Highway Administration,
*Availability, Feasibility, and Reliability of Available Nondestructive Evaluation (NDE) Technologies for Detecting and Locating Buried Utilities: Final Report*
(Washington, DC: 2023) https://doi.org/10.21949/1521981

HRDI-30/07-23(WEB)E